AN ACCURATE TIME DOMAIN INTERCONNECT MODEL OF TRANSMISSION LINE NETWORKS

by

Qingjian Yu and Ernest S. Kuh

Memorandum No. UCB/ERL M95/10

30 January 1995

AN ACCURATE TIME DOMAIN INTERCONNECT MODEL OF TRANSMISSION LINE NETWORKS

by

Qingjian Yu and Ernest S. Kuh

Memorandum No. UCB/ERL M95/10

30 January 1995

ELECTRONICS RESEARCH LABORATORY

College of Engineering
University of California, Berkeley
94720

AN ACCURATE TIME DOMAIN INTERCONNECT MODEL OF TRANSMISSION LINE NETWORKS

by

Qingjian Yu and Ernest S. Kuh

Memorandum No. UCB/ERL M95/10

30 January 1995

ELECTRONICS RESEARCH LABORATORY

College of Engineering
University of California, Berkeley
94720

An Accurate Time Domain Interconnect Model of Transmission Line Networks

Qingjian Yu *and Ernest S.Kuh
Electronics Research Lab, U.C.Berkeley

January 30, 1995

Abstract

In this paper, we present a new time domain model of interconnects modeled as transmission line networks. Each element of the characteristics of a transmission line is modeled by a principal part and a remainder. The principal part consists of an impulse and an exponential function, whose Laplace transform matches the original function at infinity frequency with order 1 and at zero frequency with order 0. The remainder in the time domain consists of a cubic polynomial for a single line and a piecewise cubic polynomial for coupled lines. The model is stable, accurate, simple and efficient to use.

1 Introduction

With the rapid increase of the signal frequency and decrease of the feature sizes in high speed electronic circuits, interconnects play increasingly important roles. On the MCM and PCB level, interconnects are modeled as transmission line networks.

Many papers have been published in the analysis of transmission line networks. As transmission lines are characterized in frequency domain and are generally terminated in nonlinear loads, a time domain model of transmission lines is needed so that convolution can be used to find the transient response. When inverse Fourier transform

*On leave from Nanjing University of Science and Technology

is directly used to find the model [2], the computation complexity will be proportional to the square of the simulation time, which is not efficient. *Padé* approximation [7] and moment matching method [8] have been used to approximate the characteristics of the line in frequency domain and then the time domain model is formed by inverse Laplace transform. While efficient recursive convolution can be accomplished by using such a model, there is no guarantee of the stability of the model, and it is difficult to predict the order of matching so that the model is accurate enough. Optimization techniques are suggested to find a good approximation in frequency domain and then transfer it into time domain [9, 4], but optimization has its known limits and it is difficult to guarantee a global rather than a local optimum unless the expensive simulated annealing is used.

In this paper, we suggest a new approach to form a simple and accurate time domain model for transmission lines. The approach consists of two steps. The first step is an approximation in the frequency domain. This is done by matching the characteristics at frequency zero with order zero (matching the value only) and at frequency ∞ with order one (matching both the value and the derivative w.r.t. $1/s$ at $s = \infty$). This approximation is designated as the principal part of the model as it approximates the original characteristic well in a wide range of high frequencies. This principal part is a first order rational function with its inverse Laplace transform consisting of an impulse and an exponential function. The main discrepancy of the approximation occurs at low frequencies. except frequency zero. The difference between the original characteristics and its principal part is called the remainder. The second step is finding the values of the remainder at sampling frequencies of interest, using the inverse FFT to find the time domain function, and fitting it with a cubic polynomial or a piecewise cubic polynomial. Thus. the time domain model of each characteristic of a line consists of an impulse, an exponential function and a number of cubic polynomials. The model is stable. simple and accurate. As recursive convolution can be easily implemented with such a model, this model is efficient to use.

This paper is organized as follows. The model of a single transmission line is presented in Sec.2. The model of coupled transmission line is presented in Sec.3. The technique of piecewise cubic fitting and the formulas of recursive convolution with cubic polynomial are presented in Sec.4 and 5, respectively. Examples and conclusions are given in Sec.6.

2 Model of single uniform line

Let r, l, c, g and d be the resistance, inductance, capacitance and conductance per unit length, and the length of a line, respectively. The telegrapher's equations of the line is as follows:

$$\frac{dV(x,s)}{dx} = -Z(s)I(x,s) \tag{1}$$

$$\frac{dI(x,s)}{dx} = -Y(s)V(x,s) \tag{2}$$

where $Z(s) = r + sl$. $Y(s) = g + sc$, and $x = 0$ and $x = d$ correspond to the near end and far end of the line, respectively.

A transmission line can be modeled by its characteristic 2 port [15] as shown in Fig.1, where $V_1(s) = V(0,s)$, $I_1(s) = I(0,s)$, $V_2(s) = V(d,s)$ and $I_2(s) = I(d,s)$. The 2-port elements are the following:

$$Z_c(s) = \sqrt{\frac{sl+r}{sc+g}} \tag{3}$$

is the characteristic impedance, and

$$W_1(s) = \Gamma(s)(2V_2(s) - W_2(s)) \tag{4}$$

$$W_2(s) = \Gamma(s)(2V_1(s) - W_1(s)) \tag{5}$$

where $\Gamma(s)$ is the propagation function, which is equal to $exp(-\theta(s)d)$ with

$$\theta(s) = \sqrt{(sl+r)(sc+g)} \tag{6}$$

The characteristic 2-port can then be described by the following equations in frequency domain:

$$V_1(s) = Z_c(s)I_1(s) + W_1(s) \tag{7}$$

and

$$V_2(s) = W_2(s) - Z_c(s)I_2(s) \tag{8}$$

Let $v_k(t), i_k(t), (k = 1,2)$, $z_c(t)$ and $\gamma(t)$ be the inverse Laplace transform of $V_k(s)$, $I_k(s)$, $Z_c(s)$ and $\Gamma(s)$, respectively. Then, the time domain characteristic 2-port model is described by the following equations:

$$v_1(t) = z_c(t) * i_1(t) + w_1(t) \tag{9}$$

$$v_2(t) = w_2(t) - z_c(t) * i_2(t) \tag{10}$$

with

$$w_1(t) = \gamma(t) * (2v_2(t) - w_2(t)) \tag{11}$$

$$w_2(t) = \gamma(t) * (2v_1(t) - w_1(t)) \tag{12}$$

where * is the symbol for convolution.

The modeling of a single line consists of the modeling of its characteristic impedance $z_c(t)$ and its propagation function $\gamma(t)$.

2.1 Model of characteristic impedance

Let $Z_c(s)$ be first approximated by $Z_{cp}(s)$, such that $Z_{cp}(0) = Z_c(0)$, $Z_{cp}(\infty) = Z_c(\infty)$ and $Z_{cp}^{(-1)} = Z_c^{(-1)}$, where $F^{(-1)} = dF(s)/d(1/s) \mid_{s\to\infty}$. [1] $Z_c(0) = \sqrt{r/g}$, $Z_c(\infty) = \sqrt{l/c}$ and $Z_c^{(-1)} = \frac{1}{2}\sqrt{\frac{l}{c}}(\frac{r}{l} - \frac{g}{c})$. Let

$$Z_{cp}(s) = \frac{a_1 s + a_0}{s + b_0} \tag{13}$$

Then, $a_1 = Z_c(\infty)$,

$$b_0 = \frac{Z_c^{(-1)}}{Z_c(0) - Z_c(\infty)} \tag{14}$$

and $a_0 = Z_c(0)b_0$. Let $z_{cp}(t) = L^{-1}Z_{cp}(s)$, then

$$z_{cp}(t) = Z_c(\infty)\delta(t) + k_z exp(-b_0 t) \tag{15}$$

where $k_z = Z_c^{(-1)}$. $z_{cp}(t)$ is the principal part of $z_c(t)$.

Let $Z_{cr}(s) = Z_c(s) - Z_{cp}(s)$ be the remainder of $Z_c(s)$. Suppose that f_0 is the basic frequency, and f_{max} is the highest frequency of interest. When the source signal is a pulse with a rising and a falling time tr and tf, respectively and assuming that

[1] We use the superscript (-1) to denote the residue of a function and the superscript -1 without paratheses to denote an inverse.

ts is the simulation time, then we choose $f_0 = 1/ts$ and $f_{max} = 2/min(tr, tf)$. Let $N = min_n\{2^n f_0 \geq f_{max}\}$. Compute $Z_{cr}(s)$ at sampling frequencies $s_k = 2\pi k f_0 j$ for k from 0 to $N-1$, and find $z_{cr}(t) = L^{-1}Z_{cr}(s)$ by inverse FFT. $z_{cr}(t)$ looks like a parabolic, and we use a cubic polynomial $z'_{cr}(t) = a_3t^3 + a_2t^2 + a_1t + a_0$ to do least square fitting for $z_r(t)$. Then, $z_c(t)$ is approximated by

$$z'_c(t) = Z_c(\infty)\delta(t) + k_z exp(-b_0t) + c_3t^3 + c_2t^2 + c_1t + c_0 \tag{16}$$

2.2 Model of propagation function

When $s \longrightarrow \infty$, $\theta(s)d \longrightarrow \tau s$ where $\tau = \sqrt{lc}d$ is the propagation delay of the line. In modeling the propagation function, we first extract τs from $\theta(s)d$ and let $\phi(s) = \theta(s)d - \tau s$. Then $\Gamma(s) = \Lambda(s)exp(-\tau s)$ with $\Lambda(s) = exp(-\phi(s))$. In so doing, for any function $x(s)$, $\Gamma(s)x(s) = \Lambda(s)exp(-\tau s)x(s)$, and correspondingly, the convolution $\gamma(t) * x(t) = \lambda(t) * x(t-\tau)$. Now we are going to approximate $\lambda(t)$.

As in the case of Sec.2.1, we first compute $\Lambda(0) = exp(-\sqrt{rg}d)$, $\Lambda(\infty) = exp(-\frac{1}{2}\tau(\frac{r}{l}+\frac{g}{c}))$ and $\Lambda^{(-1)} = \frac{1}{8}\Lambda(\infty)\tau(\frac{r}{l}-\frac{g}{c})^2$. Let the principal part of $\Lambda(s)$ be $\Lambda_p(s) = (d_1s + d_0)/(s+\epsilon_0)$. then $d_1 = \Lambda(\infty)$, $\epsilon_0 = \Lambda^{(-1)}/(\Lambda(0) - \Lambda(\infty))$ and $d_0 = \Lambda(0)\epsilon_0$. In the time domain. $\lambda_p(t) = d_1\delta(t) + k_\lambda exp(-\epsilon_0 t) = \Lambda(\infty)\delta(t) + \Lambda^{(-1)}exp(-\epsilon_0 t)$ The remainder $\lambda_r(t) = \lambda(t) - \lambda_p(t)$ is approximated by $f_3t^3 + f_2t^2 + f_1t + f_0$ in the same way as in the approximation of the remainder of the characteristic impedance. Then, $\lambda(t) \approx \lambda'(t)$ where

$$\lambda'(t) = d_1\delta(t) + k_\lambda exp(-\epsilon_0 t) + f_3t^3 + f_2t^2 + f_1t + f_0 \tag{17}$$

Example 1.

Let the frequency s be scaled by a factor ω_0 such that $s' = s/\omega_0$, and let $a = r/\omega_0 l$, $b = g/\omega_0$ and $\tau' = \tau\omega_0$, then $Z_c = Z_c(\infty)\sqrt{(s'+a)/(s'+b)}$ and $\Lambda = exp(-\tau'\sqrt{(s'+a)(s'+b)} + \tau' s')$. The accuracy of the approximation of Z_c and Λ by their principal parts depends on the ratio a/b. The near the ratio to 1, the better the approximation. We show the remainders $z_{cr}(t)$ and $\lambda_r(t)$ in Fig.2a and Fig.2b with the ratio $a/b = 10^4$. The solid lines and dashed lines correspond to the original function and their cubic polynomial fitting. respectively. It can be seen that the fitting is indeed very good.

Remarks.

1. In the case that $g = 0$, we can model $y_c(t) \equiv z_c^{-1}(t)$ instead of modeling $z_c(t)$.

2. It can be seen from Fig.2 that the curve of the remainder is dissymmetric w.r.t. the mid point. A quadratic polynomial can not fit such a curve well, so that we choose a cubic polynomial.

3. The first step of the modeling process to extract a principal part is very essential to the second step. If $z_c(t)$ or $\lambda(t)$ is obtained by directly taking the inverse FFT from $Z_c(s)$ or $\Lambda(s)$, its curve will have severe ripples. No simple polynomial or piecewise polynomial fitting can be done to approximate such a function well. Also, the numerical computation of a convolution with such a function will be very time consuming and special care must be taken to avoid excessive errors.

2.3 Time domain model of the characteristic 2-port

Now we consider the time domain model of the characteristic 2-port. Assuming that the prior simulation time is t_n and the current one is t_{n+1} with a step size $h = t_{n+1} - t_n$. We consider the the convolution $z_c(t_{n+1}) * i_1(t_{n+1})$, which is approximated by

$$z_c'(t_{n+1}) * i_1(t_{n+1}) = \int_0^{t_{n+1}} z_c'(t_{n+1} - x) i_1(x) dx =$$

$$\int_0^{t_n} z_c'(t_{n+1} - x) i_1(x) dx + \int_{t_n}^{t_{n+1}} z_c'(t_{n+1} - x) i_1(x) dx \tag{18}$$

The first term of the above expression can be computed recursively as will be described in Sec.4. Let it be expressed as $I_{1a}(t_{n+1})$. When h is small enough, the second term can be approximated by using a trapezoidal formula

$$\int_{t_n}^{t_{n+1}} z_c'(t_{n+1} - x) i_1(x) dx \approx I_{1b}(t_{n+1}) + R(h) i_1(t_{n+1}) \tag{19}$$

where $R(h) = a_1 + 0.5h(k_z + c_0)$ and $I_{1b}(t_{n+1}) = 0.5h(k_z exp(b_0 h) + c_3 h^3 + c_2 h^2 + c_1 h + c_0) i_1(t_n)$, which can also be computed. Thus, the convolution $z_c(t_{n+1}) * i_1(t_{n+1})$ can be expressed as $z(h) i_1(t_{n+1}) + e_{z1}(t_{n+1})$, where $e_{z1}(t_{n+1}) = I_{1a}(t_{n+1}) + I_{1b}(t_{n+1})$, and can be modeled by a resistance $R(h)$ and a voltage source $e_{z1}(t_{n+1})$ connected in series.

Let $y_1(t)$ be $2v_1(t) - w_1(t)$. The convolution $\gamma(t_{n+1}) * y_1(t_{n+1}) = \lambda(t_{n+1}) * y_1(t_{n+1} - \tau)$. For $t_{n+1} \le \tau$, it is zero. In the general case, it is easily computed and can be regarded as a known value. Thus, this convolution can be modeled by an independent voltage source e_{w1}.

Therefore, the time domain model of the characteristic 2-port at time t_{n+1} is a resistive two port shown in Fig.3a, where $E_{1,n+1} = e_{z1} + e_{w1}$ and $E_{2,n+1} = e_{z2} + e_{w2}$. This modeled is equivalent to the model shown in Fig.3b, where $J_{1,n+1} = E_{1,n+1}/R(h)$ and $J_{2,n+1} = E_{2,n+1}/R(h)$.

3 Model of coupled lines

In the case of a transmission line system with n coupled lines, let r, l, c and g be the resistance, inductance, capacitance and conductance matrix, respectively, and let $V(x,s)$ and $I(x,s)$ be the voltage and current vector, respectively, then the telegrapher's equations have the same forms as those of Eqs.(1) and (2). Now we consider tow kinds of its model.

3.1 Characteristic 2n-port model

Based on the above, the characteristic 2n-port of n coupled lines can also be described by Eqs.(7) and (8), and Eqs.(4) and (5) are also valid. In this case, the characteristic impedance matrix is

$$Z_c(s) = Y^{-1}(s)\sqrt{Y(s)Z(s)} \tag{20}$$

and the propagation function matrix is

$$\Gamma(s) = exp(-\sqrt{Y(s)Z(s)}d) \tag{21}$$

Let $Y(s)Z(s) = Q(s)\Theta^2(s)Q^{-1}(s)$, where $\Theta^2(s)$ is the diagonal eigen value matrix of $Y(s)Z(s)$ and $T(s)$ its corresponding eigenvector matrix. Then,

$$\Gamma(s) = Q(s)exp(-\Theta(s)d)Q^{-1}(s) \tag{22}$$

and

$$Z_c(s) = Y^{-1}(s)Q(s)\Theta(s)Q^{-1}(s) \tag{23}$$

$Z_c(0)$ can be computed by using Eq.(23). Let

$$cl = Q(\infty)T^2Q^{-1}(\infty) \tag{24}$$

where T^2 and $Q(\infty)$ are the eigenvalue and eigenvector matrix of the matrix cl, respectively. Then, from the above equations, we have

$$Z_c(\infty) = g^{-1}Q(\infty)TQ^{-1}(\infty) \tag{25}$$

The residue matrix $Z_c^{(-1)}$ cannot be computed analytically in the general case. To compute an element $Z_{cij}^{(-1)}$ of $Z_c^{(-1)}$, we select two high frequencies ω_1 and ω_2, and find $v_1 = Z_{cij}(\omega_1)$ and $v_2 = Z_{cij}(\omega_2)$. Let $u_k = imag(v_k)$ for $k = 1, 2$. Then,

$$Z_{cij}^{(-1)} = \frac{u_1\omega_1^3 - u_2\omega_2^3}{\omega_2^2 - \omega_1^2} \tag{26}$$

We can use the formulas given in Sec.(2.1) to form the principal part of each element of the characteristic impedance matrix, and then to approximate its remainder by using a piecewise cubic fitting as will be described in the next section.

Let $Q(s) = [Q_{ij}(s)]$, $Q^{-1}(s) = [R_{ij}(s)]$ and $\Theta(s) = diag[\Theta_i(s)]$, then

$$\Gamma_{ij}(s) = \sum_{k=1}^{n} S_{ijk}exp(-\Theta_k(s)d) \tag{27}$$

where $S_{ijk} = Q_{ik}R_{kj}$. Let $T = diag[\tau_k/d]$ and $\Phi_k(s) = \Theta_k - sT_k$, then

$$\Gamma_{ij}(s) = \sum_{k=1}^{n}[exp(-\tau_k s)S_{ijk}exp(-\Phi_k(s)d)] \tag{28}$$

In the general case, the n components of $\Gamma_{ij}(s)$ have different ideal delay factor $exp(-\tau_k s)$ and each of them need to be modeled individually.

From what was mentioned above, there are n^2 elements in the model of $z_c(t)$ and n^3 elements in the model of $\gamma(t)$, and there are $2(n^2 + n^3)$ convolutions to take with these two functions.

The time domain characteristic 2-port model with two coupled lines is shown in Fig.4 for illustration. In the figure, $R_{11(h)}$ and the CCVS $R_{12}I_{12,n+1}$ come from the convolution $z_{11} * i_{11} + z_{12} * i_{12}$, and the independent voltage source $E_{11,n+1}$ comes from the above convolution and the convolution $\gamma_{11} * (2v_{21} - w_{21}) + \gamma_{12} * (2v_{22} - w_{22})$. Other elements come from similar convolutions.

3.2 Model with decoupling transformation

Another way to model a system of coupled transmission lines is to use decoupling transformations and to model each decoupled single line by its characteristic 2-port

[10]. Here we follow the same idea as in [10] with a slight variation.

Let $A = Z^{1/2}YZ^{1/2} = W\Theta^2W^{-1}$ where $\Theta^2 = diag[\theta_k^2]$ is the diagonal eigenvalue matrix of A, and W is the corresponding eigenvector matrix. Let

$$X(s) = Z^{1/2}W diag[\sqrt{1/z_{0k}\theta_k}] \tag{29}$$

$$P(s) = diag[\sqrt{1/z_{0k}\theta_k}]W^{-1}Z^{1/2} \tag{30}$$

$V(x,s) = X(s)E(x,s)$ and $J(x,s) = P(s)I(x,s)$. Then, we have the decoupled system

$$\frac{dE(x,s)}{dx} = -\tilde{Z}(s)J(x,s) \tag{31}$$

$$\frac{dJ(x,s)}{dx} = -\tilde{Y}(s)E(x,s) \tag{32}$$

where $\tilde{Z}(s) = diag(z_{0k}\theta_k)$ and $\tilde{Y}(s) = diag(\theta_k/z_{0k})$. The characteristic impedance and the propagation function of the k-th decoupled line are z_{0k} and $exp(-\theta_k d)$, respectively. Note that z_{0k} can be arbitrarily chosen. For simplicity, we just choose $z_{0k} = 1$ for each k. [2]

Thus, by using the decoupling transformations, the modeling of a coupled line system can be done by modeling its decoupling transformation matrices and each of the decoupled single lines. As the characteristic impedance of each decoupled line is a constant, we only need to model its propagation function.

In the formation of the principal parts of the transformation matrices, $X(0)$ and $P(0)$ can be computed by using Eqs.(29) and (30). In order to compute their values at $s = \infty$, let $l^{1/2}cl^{1/2} \equiv B = W_\infty T^2 W_\infty^{-1}$. [3] Then,

$$X(\infty) = l^{1/2}W_\infty diag[\sqrt{d/z_{0k}\tau_k}] \tag{33}$$

and

$$P(\infty) = diag[\sqrt{d/z_{0k}\tau_k}]W_\infty^{-1}l^{1/2} \tag{34}$$

The residues $X^{(-1)}$ and $P^{(-1)}$ can be computed numerically as described in Sec.3.1.

[2] At frequencies 0 and ∞, our formulas are the same as given in [10], but at a frequency $s = j\omega$, they are different. The formulas given in [10] is based on the assumption that matrix A is real symmetric, so that matrix W is orthonormal. This is not the case when $s = j\omega$ for finite nonzero ω.

[3] The matrix T here is the same as in Eq.(24)

There are two cases encountered in the formation of the principal parts of the transformation matrices.

Case.1

In the formation of the principal part $F_p = (a_1 s + a_0)/(s + b_0)$, $b_0 = F^{(-1)}/(F(0) - F(\infty))$. In order that the model be stable, $F^{(-1)}$ and $F(0) - F(\infty)$ must have the same sign. When this condition is violated, we use a technique called shift at zero frequency (SZF) to let the principal part be $(a_1 s + a_0)/(s + b_0) - c_0/(d_1 s + 1)$. In the additional term, c_0 is so chosen that $F^{(-1)}$ and $F(0) + c_0 - F_\infty$ has the same sign and $b_0 = F^{(-1)}/(F(0) + c_0 - F(\infty))$ is positive. d_1 is set as large as possible so that the second term has no real effect on the frequency response for $f \geq f_0$ and $F^{(-1)}$ and $F(\infty)$ remain unchanged. The inverse Laplace transform of the additional term is $-c_0/d_1 exp(-t/d_1)$. As d_1 is very large, practically speaking, it can be neglected in the time domain model.

Case 2.

This case may happen in dealing with the numerical computation of residues.

Let $\omega_{max} = 2\pi f_{max}$ and $f(j\omega_{max}) = u + jv$ where u and v are real values. Then, $F(\infty) \approx u$, $F^{(-1)} \approx -v * \omega_{max}$, and the coefficient $b_0 \approx -v * \omega_{max}/(F(0) - u)$. In order that the principal part approximates $F(s)$ well in high frequencies, $| b_0 |$ should be much smaller than ω_{max}, i.e.,$| v | \ll | F(0) - F(\infty) |$ is needed. We have found that this is not always the case. When the opposite case takes place, a technique called shift at infinity frequency (SIF) similar to SZF can be used. In SIF, we modify $F_p(s)$ by subtraction of $Y(s) = q_1 s/(s + q_0)$. When $s \to \infty$, $Y(s) \to q_1$. q_1 is so chosen that $| v | \ll | F(0) - F(\infty) - q_1 |$ is satisfied. q_0 is so chosen that $| q_0 | \ll f_0$ and $L^{-1} y(s) \approx q_1 \delta(t)$.

A time domain model of a two coupled line system made from the decoupling transformation is shown in Fig.5 for illustration. In the figure, the subscript "$n + 1$" used to specify the time is omitted for brevity. The VCVS S_{11} and the independent voltage source T_{11} come from the convolution $x_{11} * e_{11} + x_{12} * e_{12}$. The CCCS J_{11} and the independent current source U_{11} come from the convolution $p_{11} * j_{11} + p_{12} * j_{12}$. R is the characteristic impedance of the decoupled lines, and W_{11} comes from the convolution $\gamma_{11} * (2e_{21} - w_{21})$. Other elements are from similar convolutions.

Now we compare the models without and with decoupling transformations, which are called model 1 and model 2 for brevity. In model 2, there are n elements in the model of propagation functions, and $2n^2$ elements in the model of transformation matrices. The number of convolution related to these elements are $2n + 4n^2$. They are about a factor of $2/n$ w.r.t. those of model 1. On the other hand, there are 6n unknowns in the circuit model with model 2 (4n voltages and 2n currents), compared with 4n unknowns (2n voltages and 2n currents) in model 1. For $n \geq 3$, the model with decoupling transformations is more efficient.

4 Piecewise cubic fitting

In the formation of the coupled line model, we use piecewise cubic fitting to approximate a remainder.

Let $f(t)$ be the function to be approximated, which is defined in the time interval $[0, t_{max}]$. Let the interval be divided into n subintervals with breaking points $0 \equiv t_0 < t_1 < t_2, \ldots < t_{n-1} < t_n \equiv t_{max}$. In the m-th subinterval $I_m = [t_{m-1}, t_m]$, suppose that $f(t)$ is approximated by $f_m(t) = a_3^m(t - t_{m-1}) + a_2^m(t - t_{m-1})^2 + a_1^m(t - t_{m-1}) + a_0^m$. For $m > 1$, we let $a_0^m = f_{m-1}(t_{m-1})$ so that the piecewise cubic polynomials are continuous at the breaking points. Let t_i^m be the i-th sampling point in the m-th subinterval. Suppose that there are s_m sampling points. Then, the least square fitting of $f_m(t)$ to $f(t)$ in the interval I_m is equivalent to finding the least square solution of the linear set of equations

$$H^m X^m = J^m \tag{35}$$

where $X^1 = [a_0^1, a_1^1, a_2^1, a_3^1]^t$ and $X^m = [a_1^m, a_2^m, a_3^m]^t$ for $m > 1$. H^1 is an $s_1 \times 4$ matrix with its element $h_{ij}^1 = (t_i^1)^{j-1}$ and J^1 is an s_1 vector with its element $J_i^1 = f(t_i^1)$. For $m > 1$, H^m is an $s^m \times 3$ matrix with its element $h_{ij}^m = (t_i^m)^j$ and the i-th element of J^m is $J_i^m = f(t_i^m) - a_0^m$. By using the Householder transformation to transform Eq.(35) to the following form

$$\begin{bmatrix} G^m \\ 0 \end{bmatrix} X^m = \begin{bmatrix} B^m \\ C^m \end{bmatrix} \tag{36}$$

where G^m is an upper triangular matrix, then X^m can be found by solving the equations $G^m X^m = B^m$.

The piecewise cubic fitting is done step by step from the first interval to the last one, and the breaking points $0 \equiv t_0 < t_1 < t_2, \ldots < t_{n-1} < t_n \equiv t_{max}$ are determined in the process one after another. We first divide the interval $[0, t_{max}]$ into p monotonic subintervals $I_1, I_2, \ldots, I_p$ with I_k defined by the terminal points $[d_{k-1}, d_k]$, where $d_0 = t_0$ and $d_p = t_{max}$. As a cubic polynomial may have at most two extremes, the initial position of the first breaking point t_1 is set in I_2 such that $t_1 = min(1.2d_1, d_2)$. Suppose that the k-th breaking point t_k is in I_j, then the initial position of the $k+1$ -th breaking point is set at $t_{k+1} = min(t_k + 1.2 * (d_j - t_k), d_{j+1}, t_{max})$. After the initial position of the breaking point of a new subinterval is set, a least square fitting is done, and the root mean square of the relative error rms is computed. If rms is within certain limit (e.g., 4% to 5.5 %), then the new breaking point is set. A farther or nearer breaking point is tried depending on the case whether rms is too small or too big. In either case, the change of the length of the subinterval is limited by a factor of 2 or 1/2, and the number of iterations is limited by 4. This process continues until the boundary of the interval is reached.

After the piecewise cubic fitting is done, the piecewise cubic polynomial is transformed into the form of $\sum_{k=0}^{m} g_k(t-t_k)1(t-t_k)$ where $g_k(t-t_k) = a_3^k(t-t_k)^3 + a_2^k(t-t^k)^2 + a_1^k(t-t_k) + a_0^k$. $1(t-t_k)$ is a unit step function starting at t_k and $a_0^k = 0$ for $k > 0$.

Example 2.

In Fig.6-8, we show an example of the remainders of the propagation functions and the elements of the decoupling matrices P and X of a two coupled line system. The solid and dashed lines correspond to the original functions and their piecewise cubic approximations. It can be seen that the approximations are quite good.

5 Recursive convolution

Each element of our model consists of an impulse, an exponential function, and a number of cubic polynomials starting at different time points. When such a function is convolved with another function $x(t)$, the convolution can be done recursively from time to time. The recursive convolution formula with an exponential function has been given in [7], and the recursive formulas with polynomials up to the order of 2 have been given in [13]. We now give the recursive formulas with a cubic polynomial for reference.

Let $f_k(t,T) = (t-T)^k 1(t-T)$ and $I_k(t,x) = f_k(t,T) * x(t) = \int_0^t (t-T-\tau)^k 1(t-T-\tau)x(\tau)d\tau$. Then, for the time $t+h > T$, when trapezoidal formula is used to do integration, we have the recursive formulas for the convolution from k=0 to 3 as follows:

$$I_0(t+h,x) = I_0(t,x) + 0.5h(x(t-T) + x(t+h-T)),$$
$$I_1(t+h,x) = I_1(t,x) + hI_0(t,x) + 0.5h^2x(t-T),$$
$$I_2(t+h,x) = I_2(t,x) + 2hI_1(t,x) + h^2I_0(t,x) + 0.5h^3x(t-T),$$
$$I_3(t+h,x) = I_3(t,x) + 3hI_2(t,x) + 3h^2I_1(t,x) + h^3I_0(t,x) + 0.5h^4x(t-T).$$

Note that when $T > 0$, these convolutions have no relation with the current value of x. i.e.. x(t+h): and when $T = 0$, only $I_0(t+h,x)$ has a term related to $x(t+h)$.

6 Examples and conclusion

We present two examples to show the simulation results with our model. The first example is a single line circuit shown in Fig.9, with the line voltages shown in Fig.10. The second example is a two-coupled line circuit shown in Fig.11, with the line voltages shown in Fig.12. The solid lines correspond to the simulation results by using our model and the recursive convolution, while the dashed lines (with an extension ".fft") correspond to those obtained by directly using FFT and exact expressions of the characteristics of the lines. It can be seen that these two results match very well, which shows the accuracy of our model.

We also test the case when the remainders of the characteristics are not approximated by piecewise cubic polynomial so that no recursive convolution can be used. The CPU time is almost 100 times more than using our model with recursive convolution, which shows the efficiency of our model.

We have presented a new time domain model for single and coupled transmission lines. The model of each element consists of an impulse function, an exponential function, and a piecewise cubic polynomial. The model is stable. As very good approximation can be obtained in the piecewise cubic polynomial fitting for the remainders, the model can be very accurate. In fact, as the principal part approximates the characteristic well in a wide frequency region, the remainder is relatively small and only a few pieces of piecewise cubic polynomials can lead to very good accuracy. Therefore, the model is both simple and accurate. As the model is compatible with recursive convolution, it is efficient in the use of time domain simulation. Compared with the model formed by using least square fitting in frequency domain only, our model is easier to form and computationally inexpensive. Our future work is to extend our model to nonuniform and frequency-dependent lines.

References

[1] A.Deutsch et al. "High-speed signal propagation on lossy transmission lines," IBM J. Res. & Dev., vol.34, No.4, pp.601-615, July 1990.

[2] J.E.Schutt-Aine, "Transient analysis of nonuniform transmission lines," IEEE Trans. on CAS-I. vol.39, No.5, pp.378-385, May 1992.

[3] H.Grabinski. "An algorithm for computing the signal propagation on lossy VLSI interconnect system in the time domain," INTEGRATION, vol.7, pp.35-48, 1989.

[4] E.C.Chang and S.M.Kang, "Computationally efficient simulation of a lossy transmission line with skin effect by using numerical inversion of Laplace transform," IEEE Trans. on CAS-I, vol.39, No.11, pp.861-868, No. 1992.

[5] R.Griffith et al, "A CAD framework for simulation and optimization of high-speed VLSI interconnects," IEEE Trans. on CAS-I, vol.39, No.11, pp.893-906, Nov. 1992.

[6] V.K.Tripathi and N.Orhanovic, "Time-domain characterization and analysis of dispersive dissipative interconnects," IEEE Trans. on CAS-1, vol.39, No.11, pp.938-945. Nov. 1992.

[7] S.Lin and E.S.Kuh, "Transient simulation of lossy interconnects based on the recursive convolution formulation," IEEE Trans. on ACS-I, vol.39, No.11, pp.879-892, Nov. 1992.

[8] J.E.Bracken et al,"Interconnect simulation with asymptotic waveform evaluation (AWE)," IEEE Trans. on CAS-I, vol.39, No.11, pp.869- 878, Nov. 1992.

[9] F.Y.Chang, "Waveform relaxation analysis of nonuniform lossy transmission lines characterized with frequency-dependent parameters," IEEE Trans. on CAS, vol.38, No.12, pp.1484-1500, Dec. 1991.

[10] F.Y.Chang and O.Wing, "Transient simulation of lossy coupled transmission lines characterized with frequency-dependent parameters," International Journal of High Speed Electronics, Vol.2, No.4, 319-353, 1991.

[11] D.S.Gao et al. "Modeling and simulation of interconnection delays and crosstalks in high-speed integrated circuits," IEEE Trans. on CAS, vol.37, No.1, pp.1-9, Jan. 1990.

[12] C.Gordan et al. "Time-domain simulation of multiconductor lines with frequency-dependent losses." IEEE Trans. on CAD, vol.11, No.11, pp.1372-1387, Nov. 1992.

[13] E.C.Chang and S.M.Kang. "Transient Simulation of Lossy Transmission Lines Using Piecewise Recursive Convolution," Proc. 1993 Int. Symp. on Nonlinear Theory and its Applications, vol.1, 2.6.3, Dec. 1993.

[14] Q.Yu and O.Wing. "Computational models of transmission lines with skin effects and dielectric loss," IEEE Trans. on CAS-I, vol.41, No.2, pp. , Feb. 1994.

[15] F.H.Branin, "Transient analysis of lossless transmission lines," Proc. IEEE, vol.55, pp.2012-2013, Nov. 1967.

Captions of Figures 2, 6,7,8, 10 and 12

Fig.2 Remainders of characteristic impedance and propagation function of a single line

Fig.6 Remainders of propagation function of two coupled lines

Fig.7 Remainders of decoupling transformation matrix X of two coupled lines

Fig.8 Remainders of decoupling transformation matrix P of two coupled lines

Fig.10 Simulation result of a single line circuit

Fig.12 Simulation result of two coupled line circuit

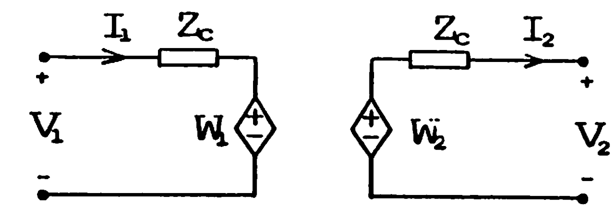

Fig.1

Characteristic 2-port

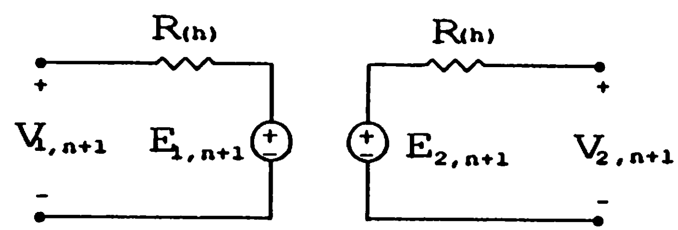

a

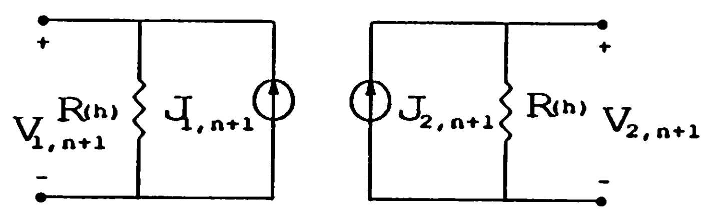

b

Fig.3

Time-domain Model of characteristic 2-port

Fig.2a

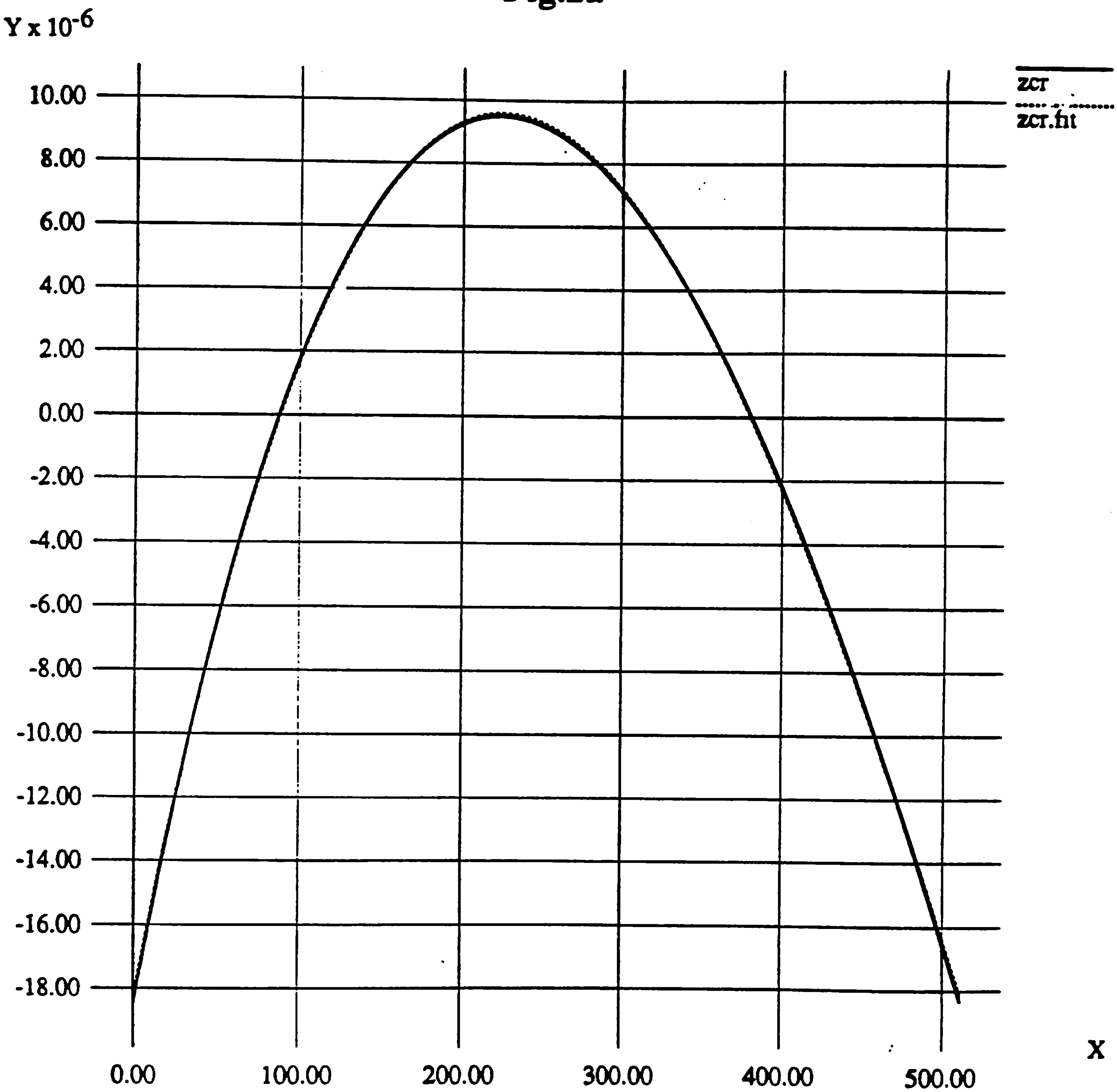

Y x 10-6
10.00
8.00
6.00
4.00
2.00
0.00
-2.00
-4.00
-6.00
-8.00
-10.00
-12.00
-14.00
-16.00
-18.00
0.00
100.00
200.00
300.00
400.00
500.00
X
zcr
zcr.fit

Fig.2b

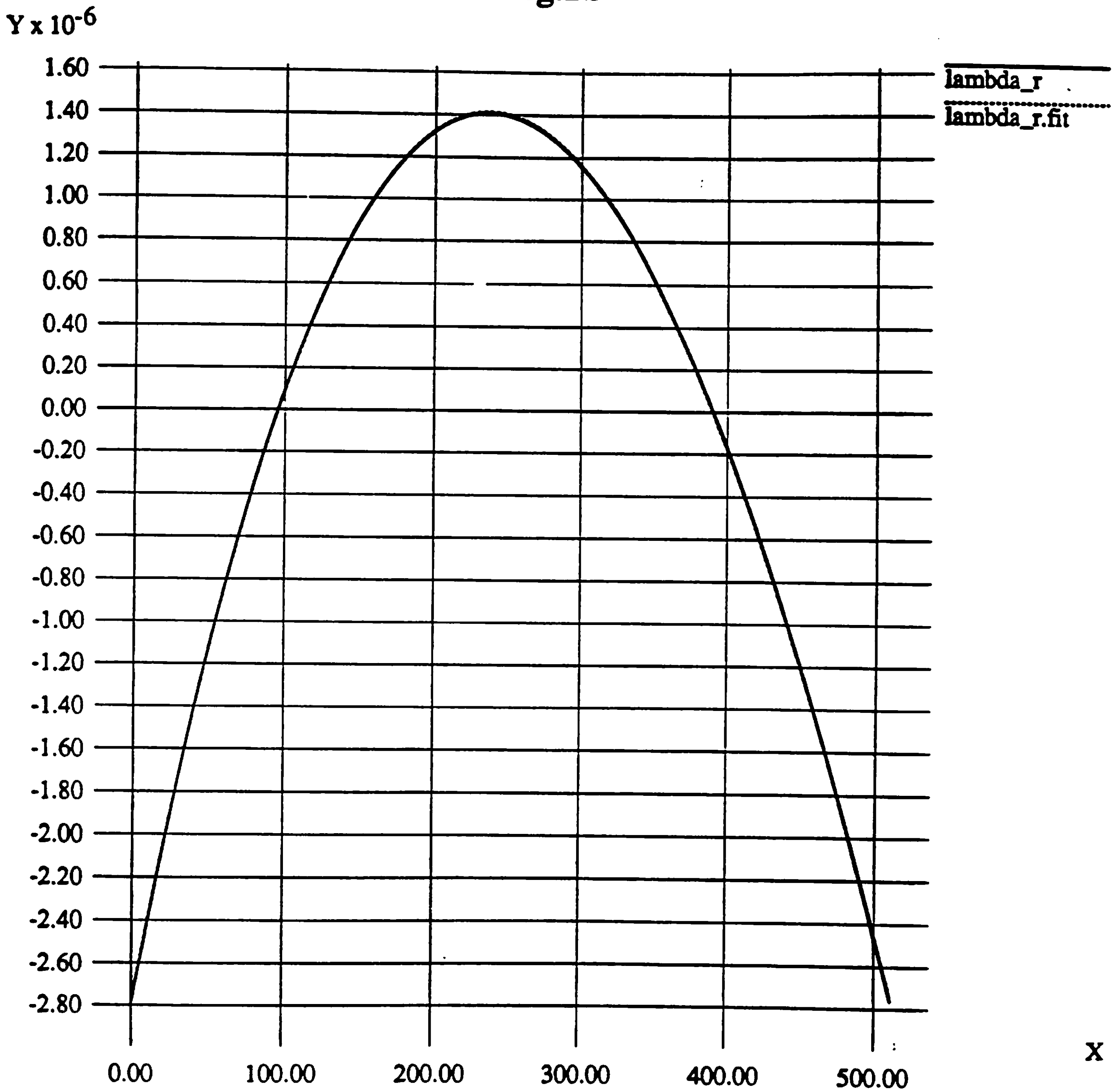
Y x 10-6
1.60
1.40
1.20
1.00
0.80
0.60
0.40
0.20
0.00
-0.20
-0.40
-0.60
-0.80
-1.00
-1.20
-1.40
-1.60
-1.80
-2.00
-2.20
-2.40
-2.60
-2.80
lambda_r
lambda_r.fit
0.00
100.00
200.00
300.00
400.00
500.00
X

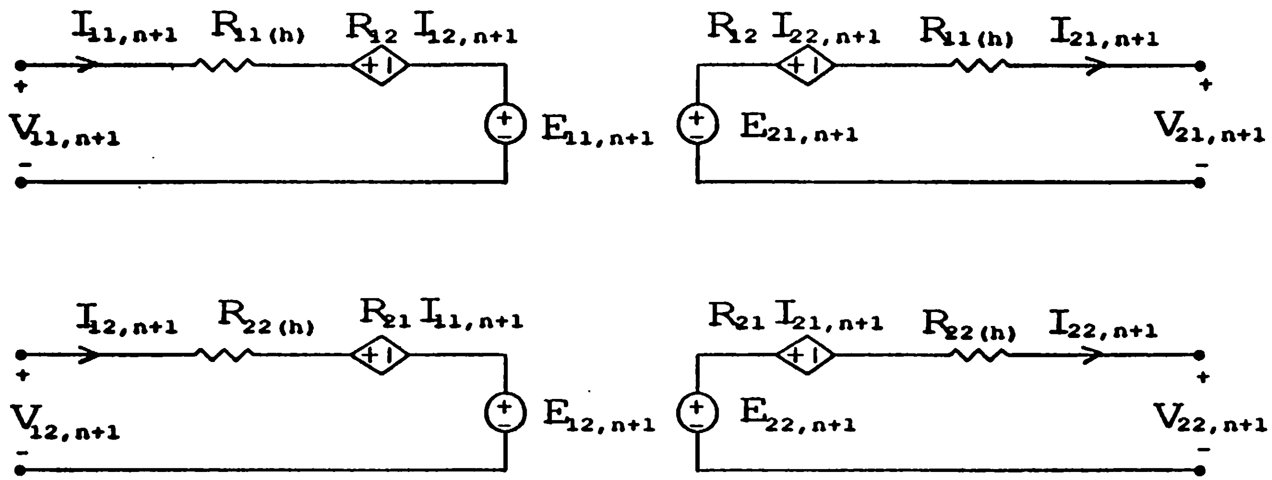

Fig.4

Time-domain model of characteristic

2-port of two coupled lines

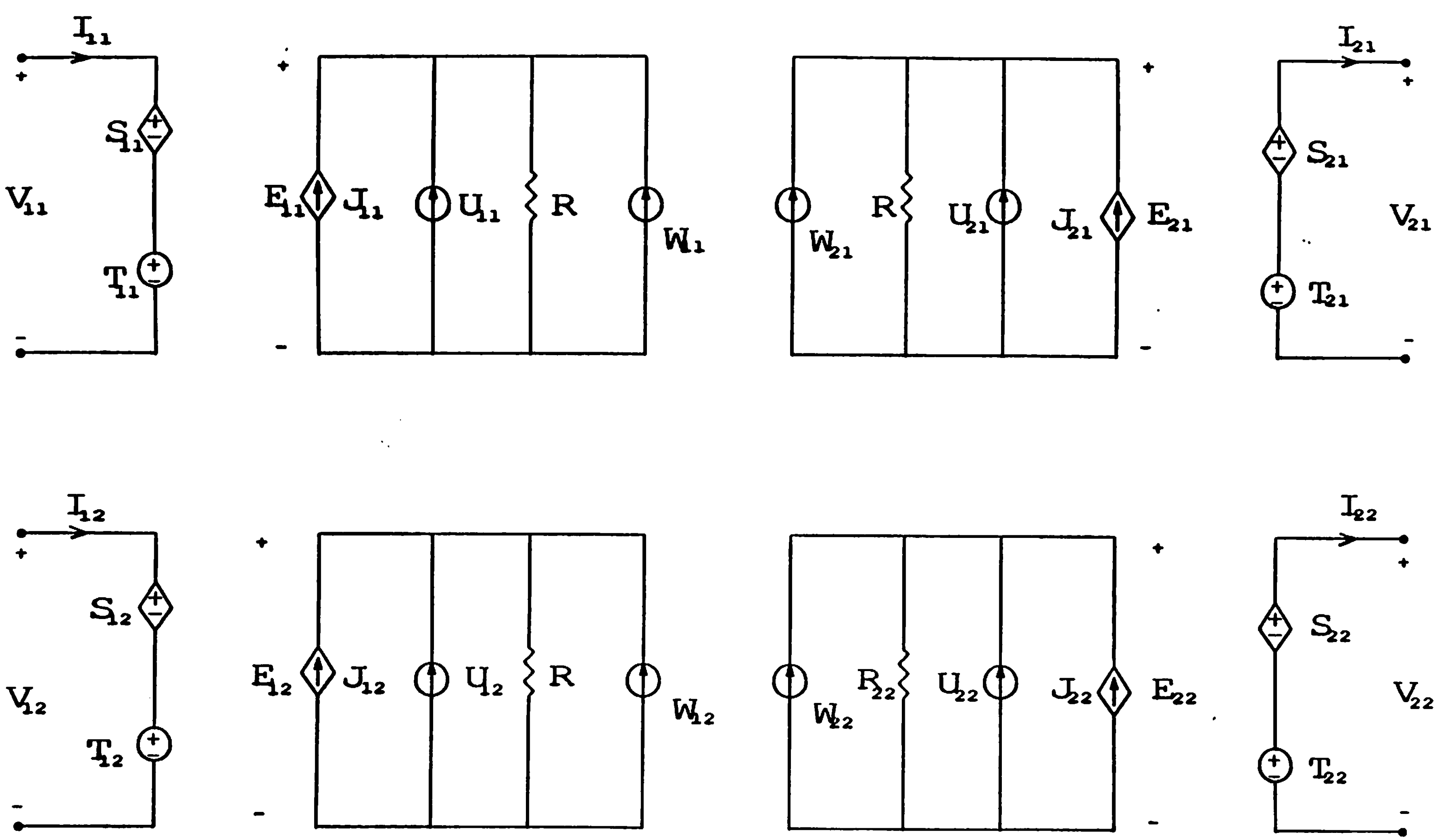

Fig.5 Time-domain model of 2-coupled lines

by decoupling transformation

Fig.6a

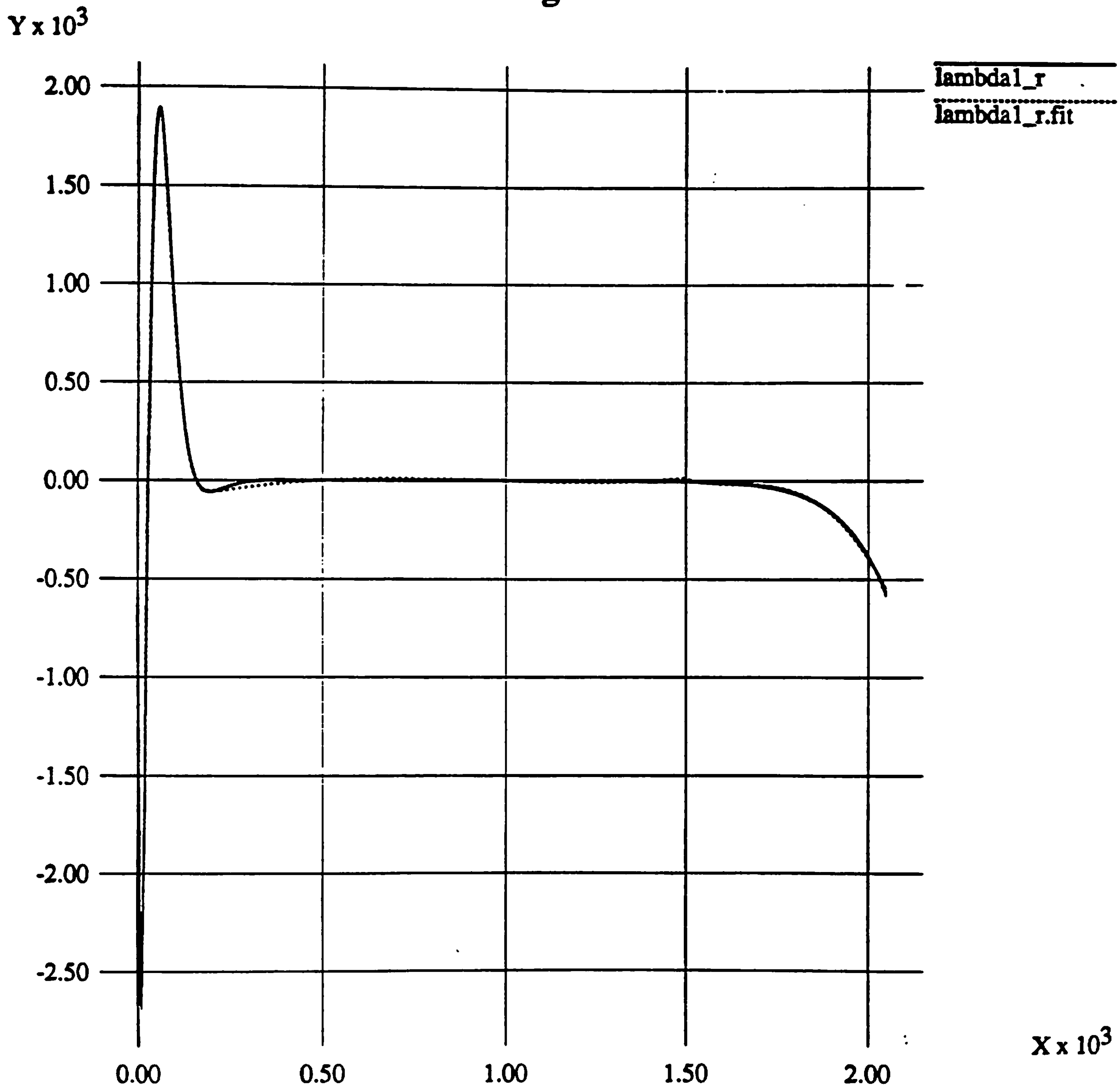
Y x 10^3
2.00
1.50
1.00
0.50
0.00
-0.50
-1.00
-1.50
-2.00
-2.50
0.00
0.50
1.00
1.50
2.00
X x 10^3
lambda1_r
lambda1_r.fit

Fig.6b

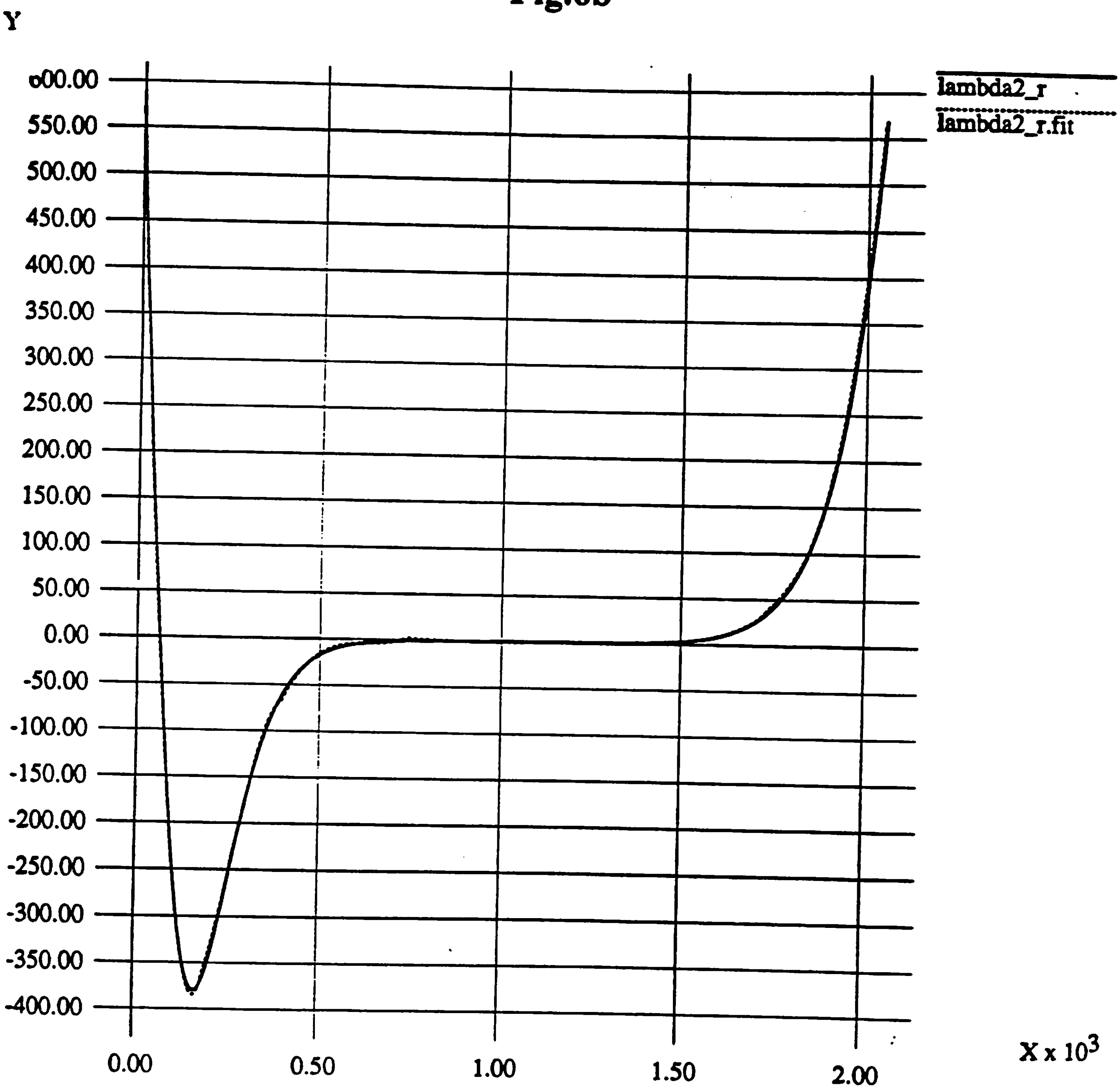
Y
600.00
550.00
500.00
450.00
400.00
350.00
300.00
250.00
200.00
150.00
100.00
50.00
0.00
-50.00
-100.00
-150.00
-200.00
-250.00
-300.00
-350.00
-400.00
0.00
0.50
1.00
1.50
2.00
X x 10^3
lambda2_r
lambda2_r.fit

Fig.7a

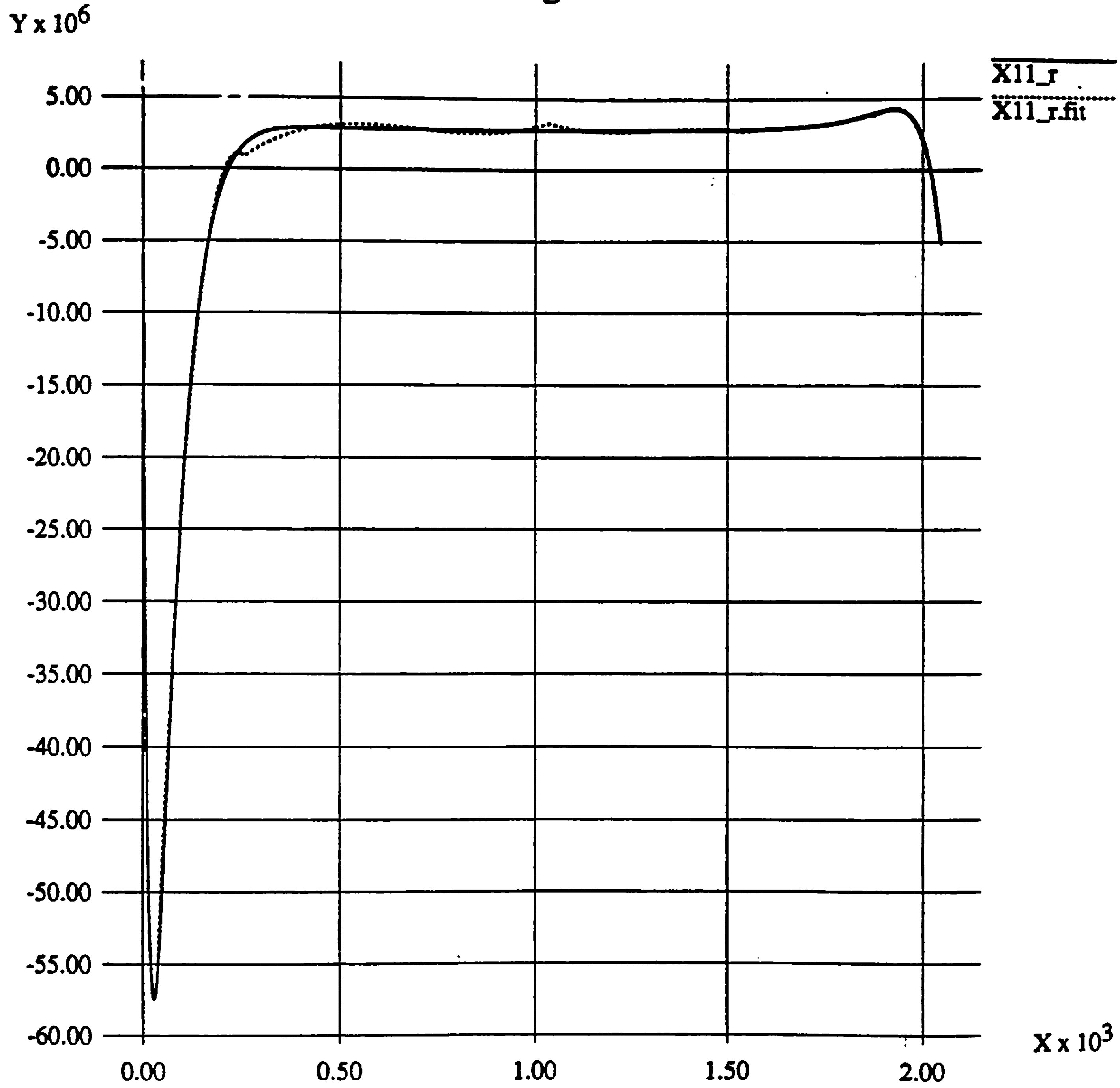
Y x 10^6
X11_r
X11_r.fit
5.00
0.00
-5.00
-10.00
-15.00
-20.00
-25.00
-30.00
-35.00
-40.00
-45.00
-50.00
-55.00
-60.00
X x 10^3
0.00
0.50
1.00
1.50
2.00

Fig.7b

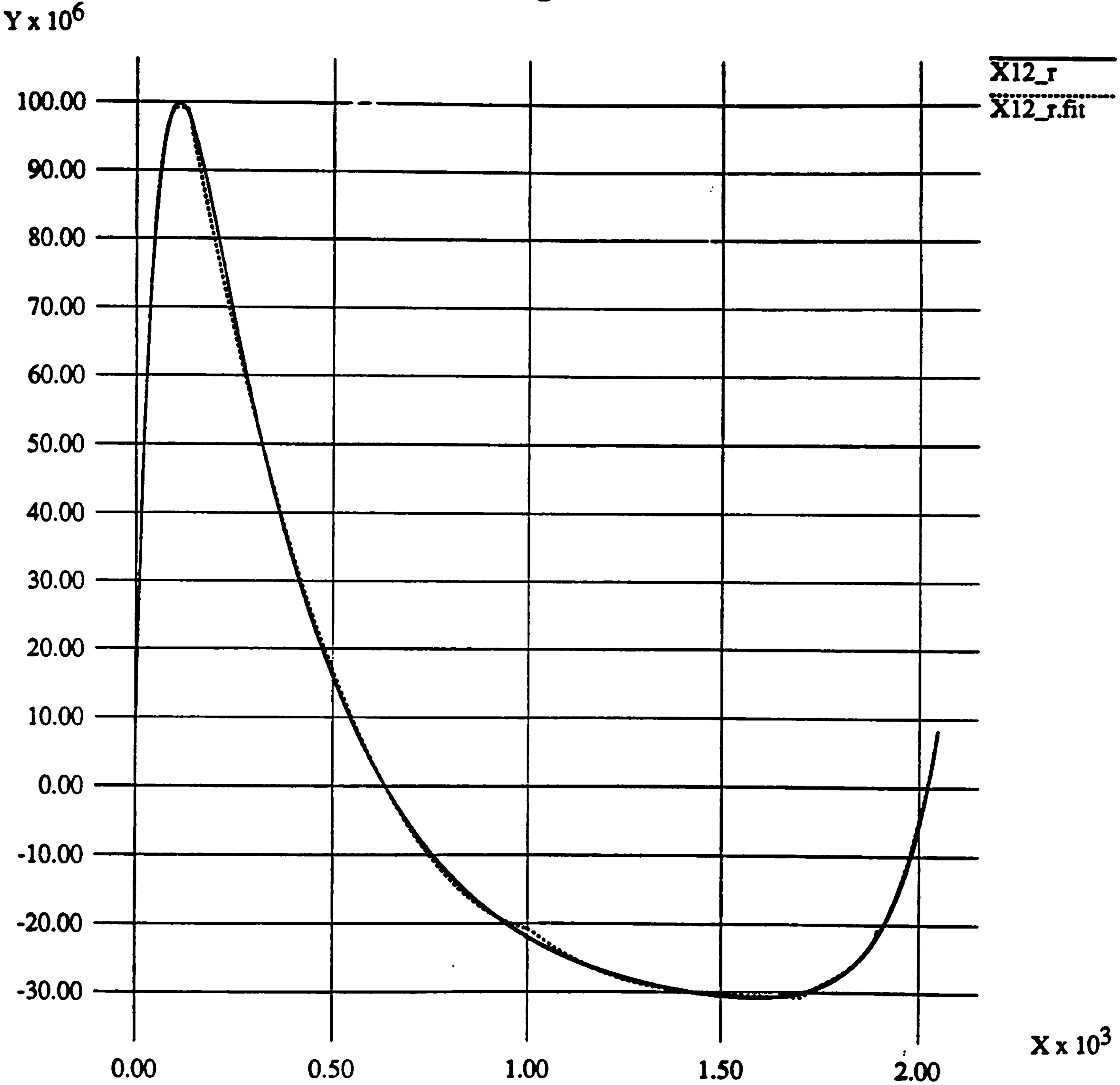
Y x 10^6
X12_r
X12_r.fit
100.00
90.00
80.00
70.00
60.00
50.00
40.00
30.00
20.00
10.00
0.00
-10.00
-20.00
-30.00
0.00
0.50
1.00
1.50
2.00
X x 10^3

Fig.7c

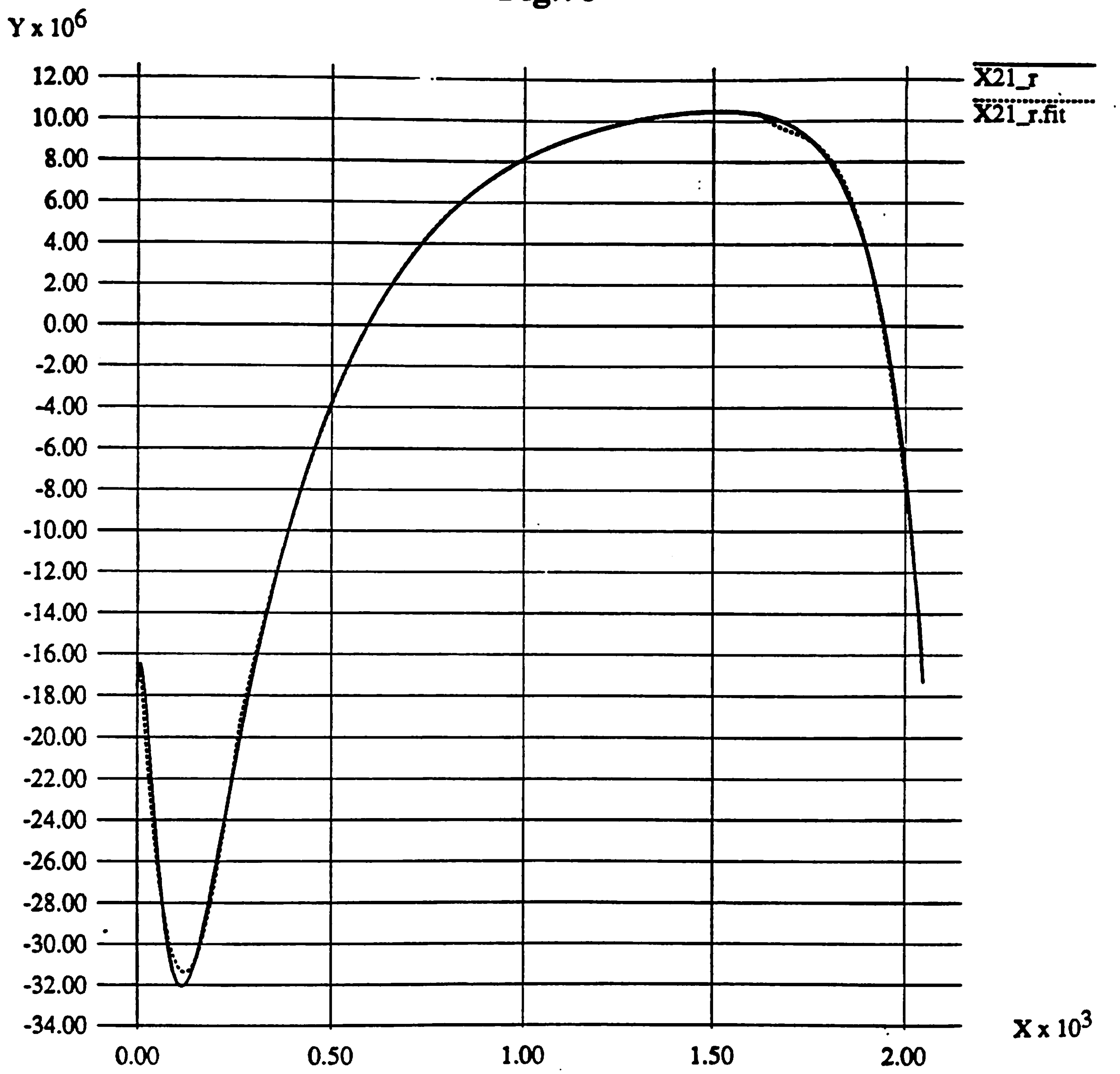
Y x 10^6
12.00
10.00
8.00
6.00
4.00
2.00
0.00
-2.00
-4.00
-6.00
-8.00
-10.00
-12.00
-14.00
-16.00
-18.00
-20.00
-22.00
-24.00
-26.00
-28.00
-30.00
-32.00
-34.00
0.00
0.50
1.00
1.50
2.00
X x 10^3
X21_r
X21_r.fit

Fig.7d

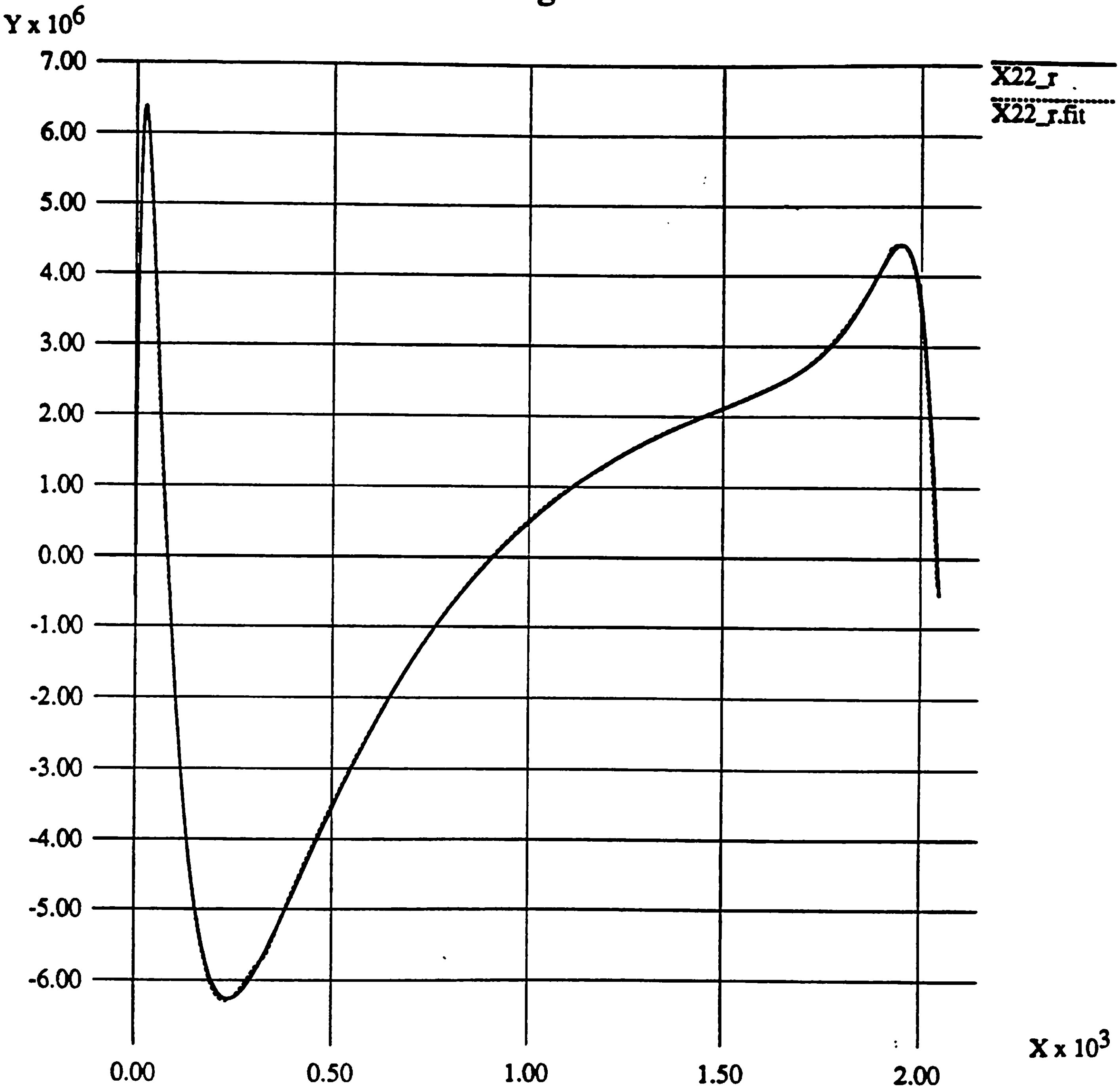

Y x 10^6
7.00
6.00
5.00
4.00
3.00
2.00
1.00
0.00
-1.00
-2.00
-3.00
-4.00
-5.00
-6.00
X22_r
X22_r.fit
0.00
0.50
1.00
1.50
2.00
X x 10^3

Fig.8a

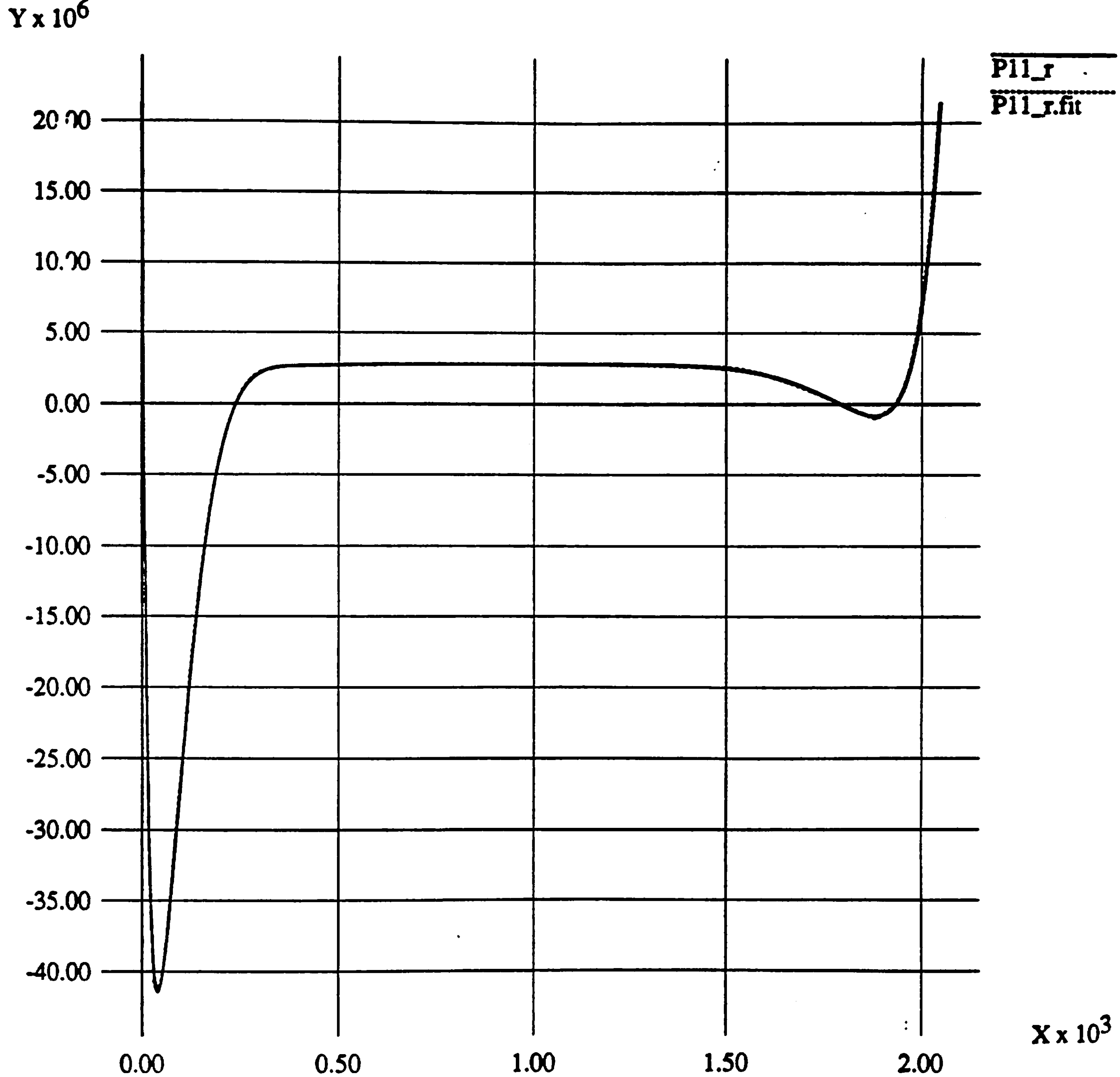

Y x 10^6
P11_r
P11_r.fit
20.00
15.00
10.00
5.00
0.00
-5.00
-10.00
-15.00
-20.00
-25.00
-30.00
-35.00
-40.00
0.00
0.50
1.00
1.50
2.00
X x 10^3

Fig.8b

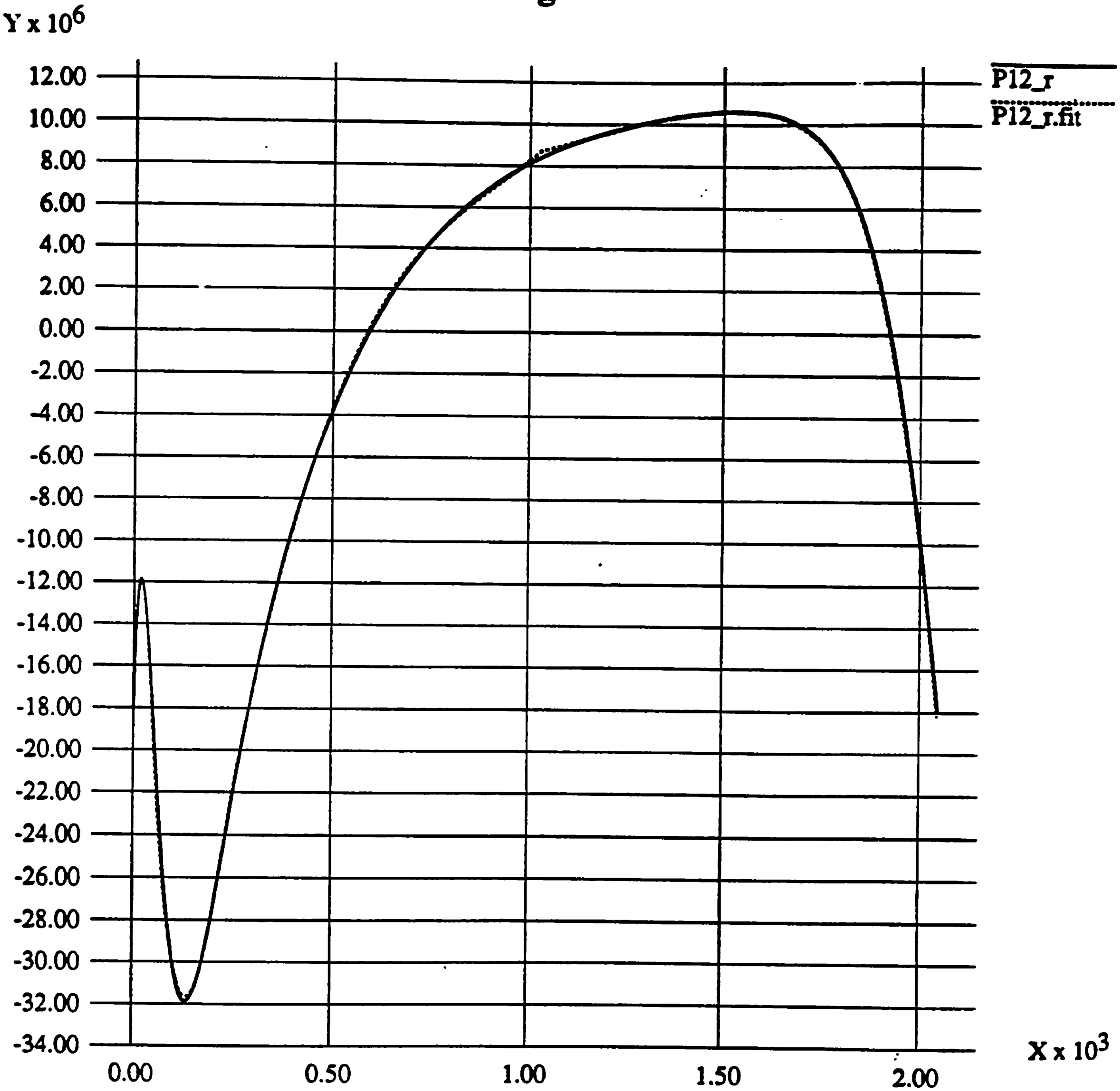

Y x 10^6
12.00
10.00
8.00
6.00
4.00
2.00
0.00
-2.00
-4.00
-6.00
-8.00
-10.00
-12.00
-14.00
-16.00
-18.00
-20.00
-22.00
-24.00
-26.00
-28.00
-30.00
-32.00
-34.00
0.00
0.50
1.00
1.50
2.00
X x 10^3
P12_r
P12_r.fit

Fig.8c

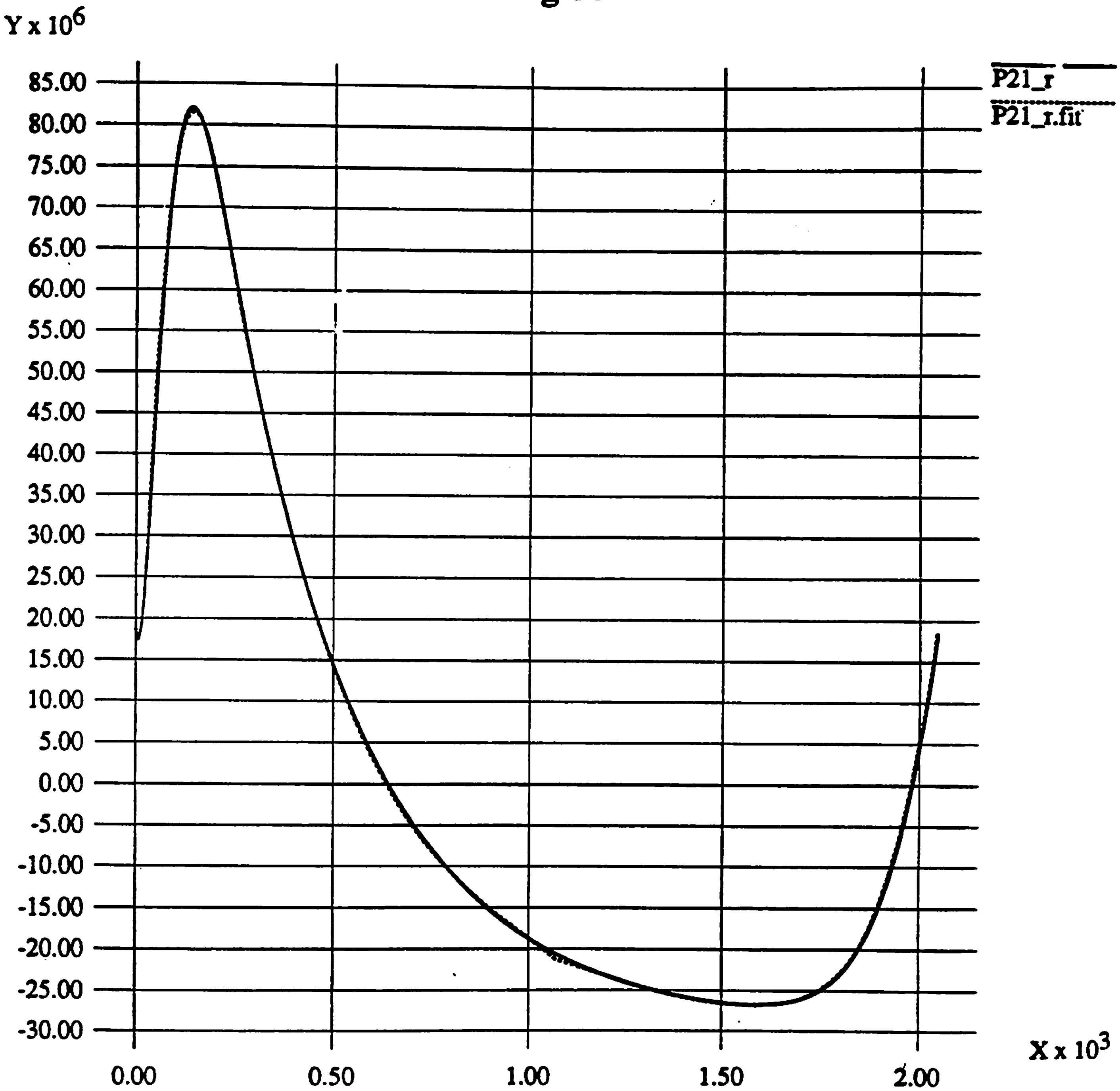
Y x 10^6
85.00
80.00
75.00
70.00
65.00
60.00
55.00
50.00
45.00
40.00
35.00
30.00
25.00
20.00
15.00
10.00
5.00
0.00
-5.00
-10.00
-15.00
-20.00
-25.00
-30.00
0.00
0.50
1.00
1.50
2.00
X x 10^3
P21_r
P21_r.fit

Fig.8d

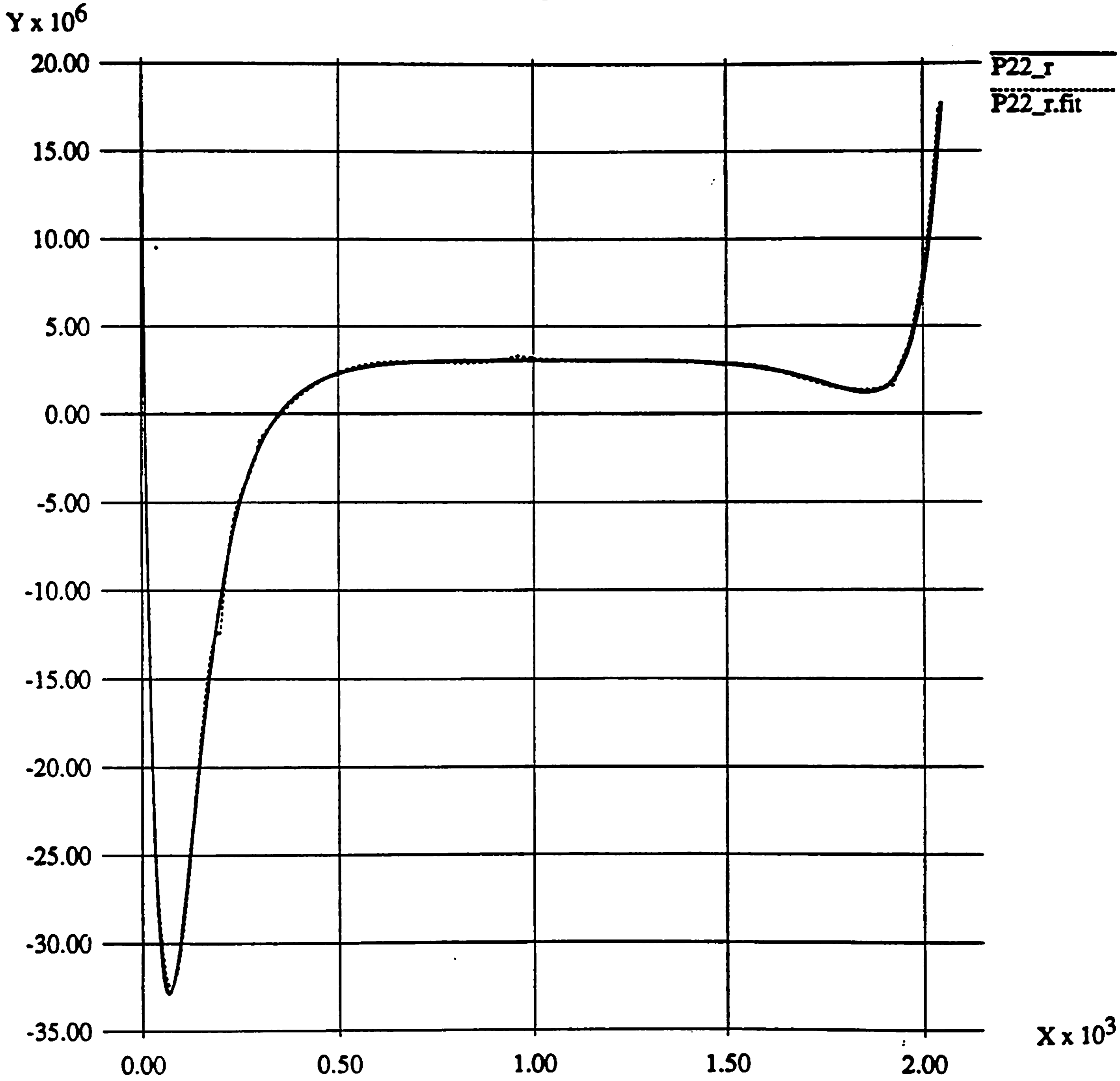
Y x 10^6
20.00
15.00
10.00
5.00
0.00
-5.00
-10.00
-15.00
-20.00
-25.00
-30.00
-35.00
P22_r
P22_r.fit
0.00
0.50
1.00
1.50
2.00
X x 10^3

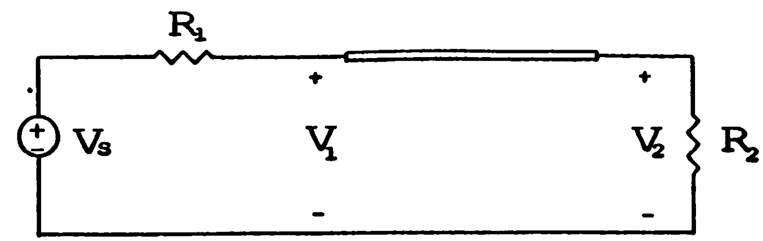

Fig.9 Test Circuit of Example 3

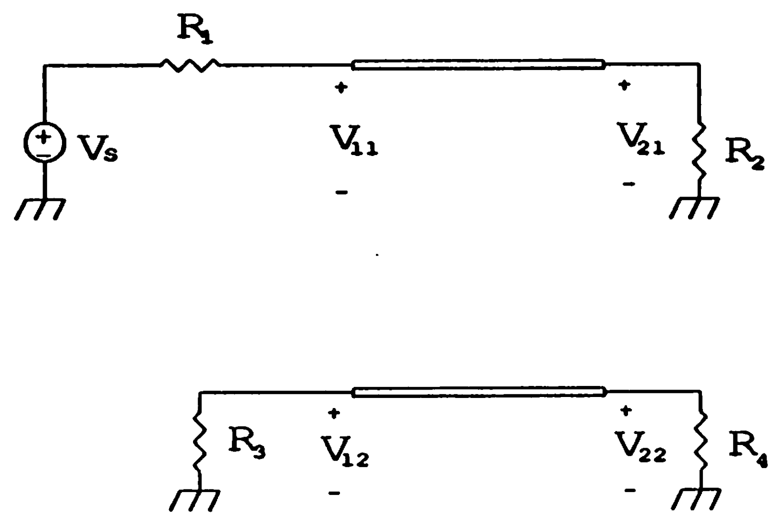

Fig.11 Test circuit of Example 4

Fig.10a

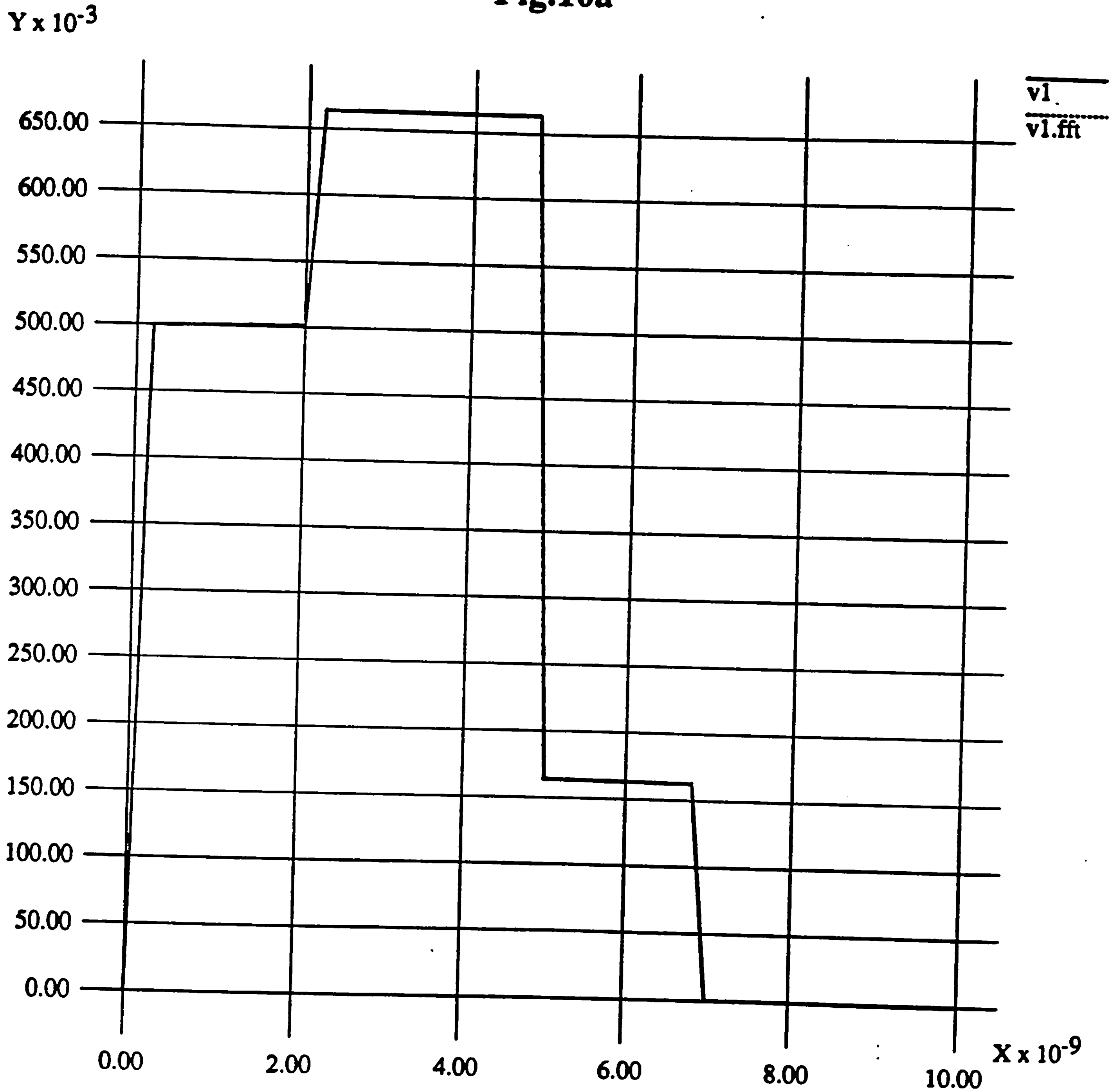
Y x 10^-3
650.00
600.00
550.00
500.00
450.00
400.00
350.00
300.00
250.00
200.00
150.00
100.00
50.00
0.00
0.00
2.00
4.00
6.00
8.00
10.00
X x 10^-9
v1
v1.fft

Fig.10b

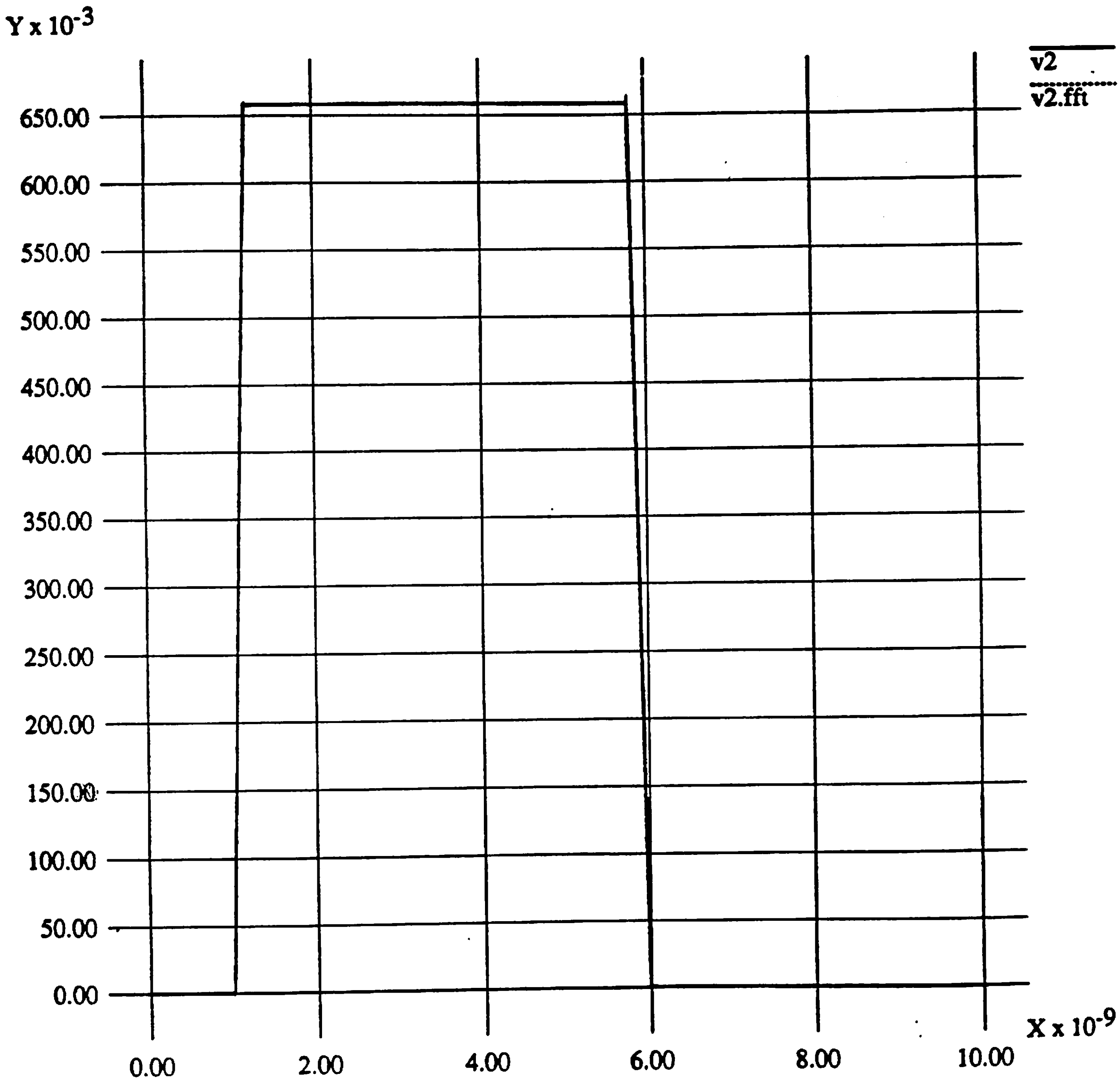
Y x 10^-3
v2
v2.fft
650.00
600.00
550.00
500.00
450.00
400.00
350.00
300.00
250.00
200.00
150.00
100.00
50.00
0.00
0.00
2.00
4.00
6.00
8.00
10.00
X x 10^-9

Fig.12a

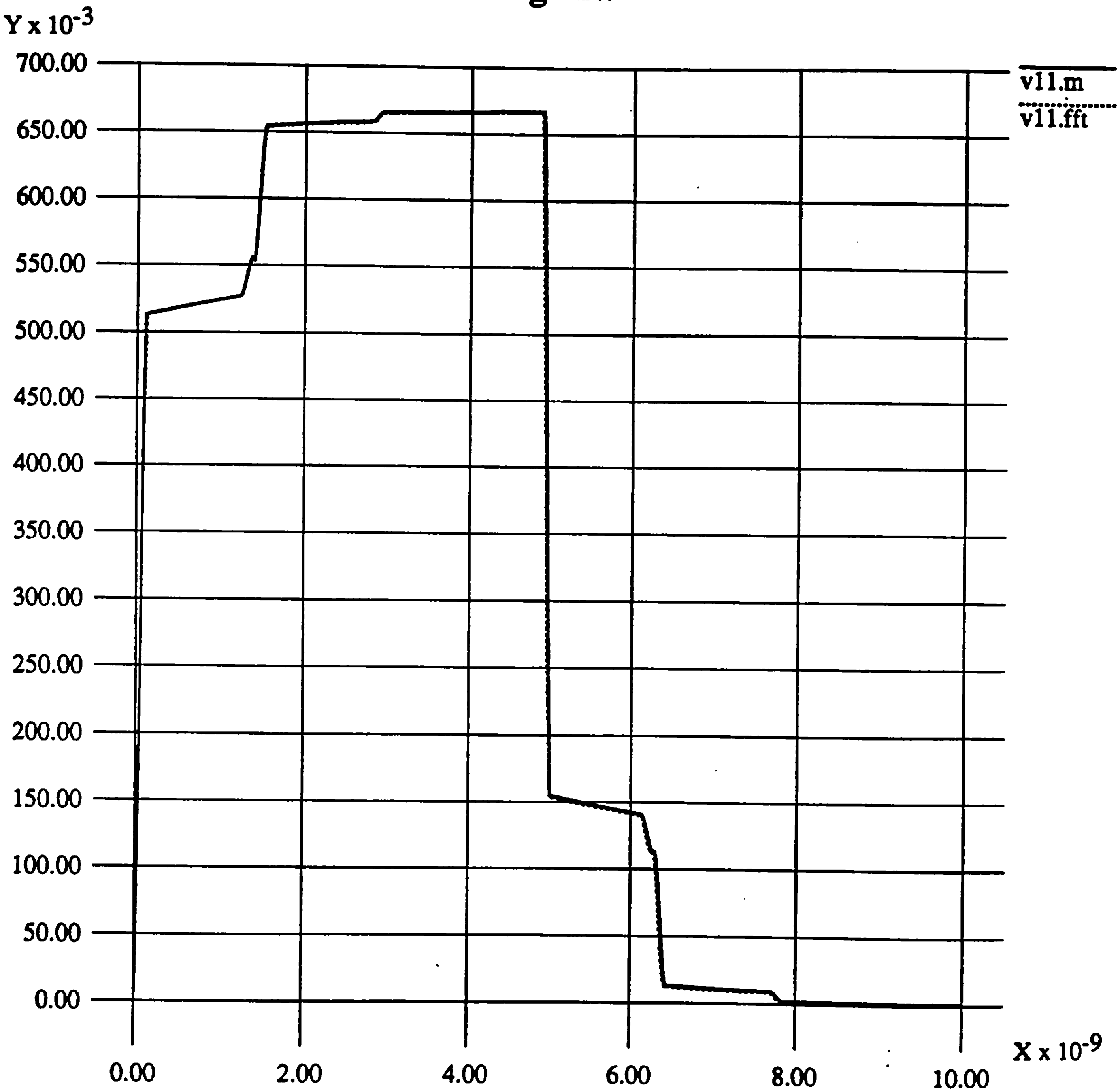
Y x 10^{-3}
700.00
650.00
600.00
550.00
500.00
450.00
400.00
350.00
300.00
250.00
200.00
150.00
100.00
50.00
0.00
0.00
2.00
4.00
6.00
8.00
10.00
X x 10^{-9}
v11.m
v11.fft

Fig.12b

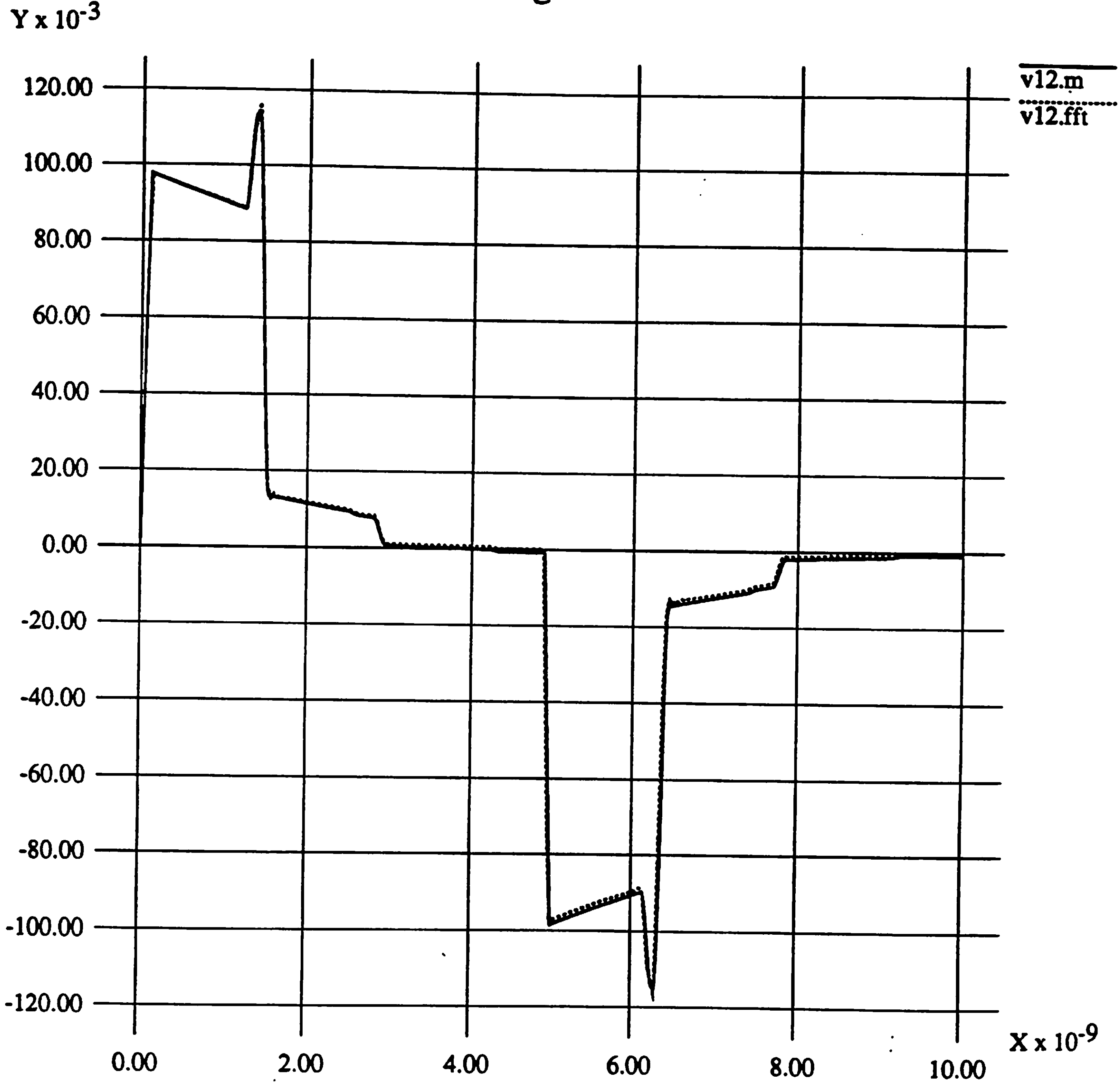
Y x 10-3
120.00
100.00
80.00
60.00
40.00
20.00
0.00
-20.00
-40.00
-60.00
-80.00
-100.00
-120.00
0.00
2.00
4.00
6.00
8.00
10.00
X x 10-9
v12.m
v12.fft

Fig.12c

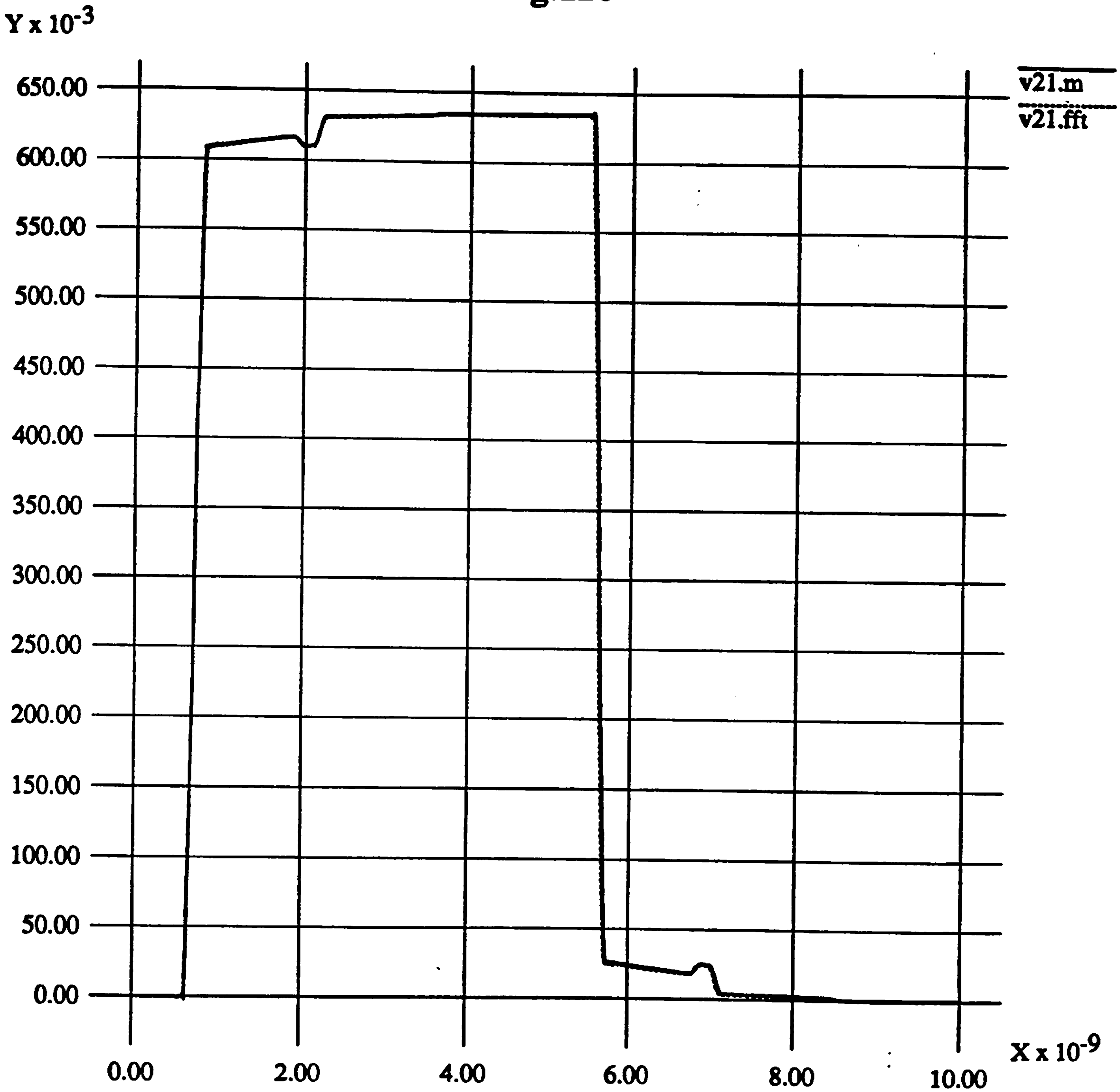

Y x 10^-3
650.00
600.00
550.00
500.00
450.00
400.00
350.00
300.00
250.00
200.00
150.00
100.00
50.00
0.00
0.00
2.00
4.00
6.00
8.00
10.00
X x 10^-9
v21.m
v21.fft

Fig.12d

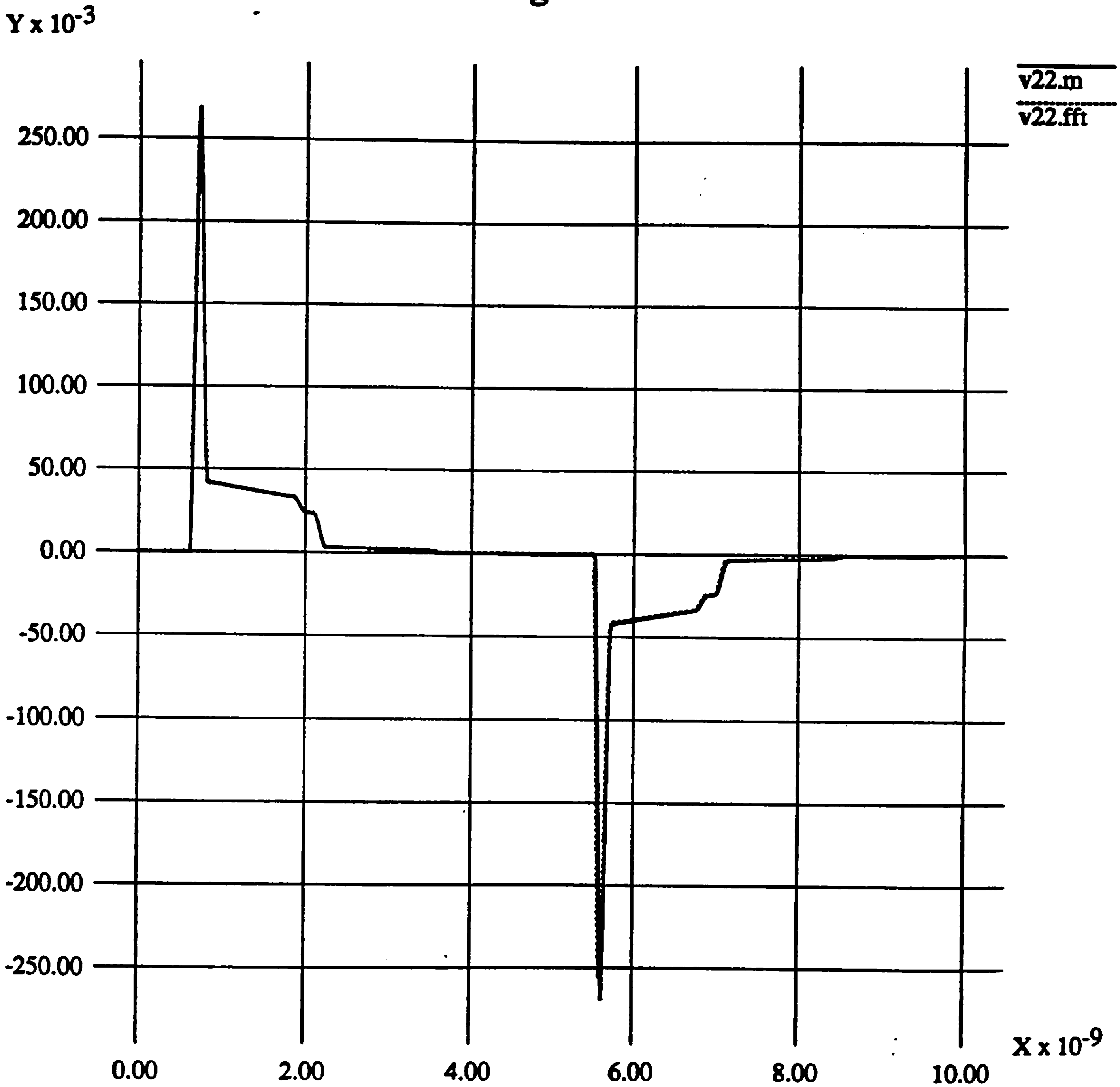
Y x 10^-3
v22.m
v22.fft
250.00
200.00
150.00
100.00
50.00
0.00
-50.00
-100.00
-150.00
-200.00
-250.00
0.00
2.00
4.00
6.00
8.00
10.00
X x 10^-9